Condensin IDC, H4K20me1, and perinuclear tethering maintain X chromosome repression in C. elegans Jessica Trombley, Audry I. Rakozy, Eshna Jash, Györgyi Csankovszki* Department of Molecular, Cellular, and Developmental Biology, University of Michigan, Ann Arbor, Michigan, United States of America *corresponding author e-mail: gyorgyi@umich.edu

Abstract

Dosage compensation in *Caenorhabditis elegans* equalizes X-linked gene expression between XX hermaphrodites and XO males. The process depends on a condensin-containing dosage compensation complex (DCC), which binds the X chromosomes in hermaphrodites to repress gene expression. Condensin IDC and an additional five DCC components must be present on the X during early embryogenesis in hermaphrodites to establish dosage compensation. However, whether the DCC's continued presence is required to maintain the repressed state once established is unknown. Beyond the role of condensin I^{DC} in X chromosome compaction, additional mechanisms contribute to X-linked gene repression. DPY-21, a non-condensin I^{DC} DCC component, is an H4K20me2/3 demethylase whose activity enriches the repressive histone mark, H4 lysine 20 monomethylation, on the X chromosomes. In addition, CEC-4 tethers H3K9me3-rich chromosomal regions to the nuclear lamina, which also contributes to X-linked gene repression. To investigate the necessity of condensin I^{DC} during the larval and adult stages of hermaphrodites, we used the auxin-inducible degradation system to deplete the condensin IDC subunit DPY-27. While DPY-27 depletion in the embryonic stages resulted in lethality, DPY-27 depleted larvae and adults survive. In these DPY-27 depleted strains, condensin IDC was no longer associated with the X chromosome, the X became decondensed, and the H4K20me1 mark was gradually lost, leading to X-linked gene derepression. These results suggest that the stable maintenance of dosage compensation requires the continued presence of condensin I^{DC}. A loss-of-function mutation in cec-4, in addition to the depletion of DPY-27 or the genetic mutation of dpy-21, led to even more significant increases in X-linked gene expression, suggesting that tethering heterochromatic regions to the nuclear lamina helps stabilize repression mediated by condensin I^{DC} and H4K20me1.

47 Author Summary

In some organisms, whether an individual becomes male, female, or hermaphrodite is determined by the number of their sex chromosomes. In the nematode *Caenorhabditis elegans*, males have one X chromosome, whereas hermaphrodites have two X chromosomes. This difference in the number of X chromosomes is crucial for deciding whether an individual becomes a hermaphrodite or a male. However, having two X chromosomes can lead to problems because it results in different gene expression levels, resulting in hermaphrodite lethality. To solve this issue, many organisms undergo a process called dosage compensation. Dosage compensation in *C. elegans* is achieved by a group of proteins known as the dosage compensation complex (DCC), which includes a protein called DPY-27. The function of DPY-27 is essential during early embryonic development. This study shows that in contrast to early embryonic development, larvae and adults can still survive when DPY-27 is missing. In these worms, all known mechanisms involved in dosage compensation are disrupted and the X is no longer repressed. Our results suggest that the maintenance of dosage compensation in nematodes is an active process, and that it is essential for survival

when the organism is developing, but once fully developed, the process becomes dispensable.

Introduction

- 66 Chromosome conformation, subnuclear localization, and the post-translational
- 67 modifications of histones are closely linked to gene expression. The relationship
- between these processes plays a crucial role in an organism's development, growth,
- and survival. Dosage compensation in the nematode Caenorhabditis elegans offers an
- 70 excellent paradigm for exploring chromosome-wide gene regulation.
- 71 There is an inherent imbalance in chromosomal gene expression in species with
- heterogametic sexes [1]. As in numerous other species with chromosome-based sex
- 73 determination, C. elegans has evolved several molecular mechanisms to ensure equal
- 74 gene expression from the sex chromosomes between the sexes [2]. This process is
- 75 known as dosage compensation. In *C. elegans*, hermaphrodites have two X
- 76 chromosomes (2X:2A), whereas males have only one X and no other sex chromosome
- 77 (1X:2A) [3]. This difference in chromosome count is essential for sex determination
- 78 [3,4]. However, without correction, in hermaphrodites, transcription from the X doubles
- relative to males, leaving the hermaphrodite population inviable [5]. The dosage
- 80 compensation mechanism in *C. elegans* corrects for the differing numbers of sex
- 81 chromosomes by reducing the gene expression of the hermaphrodite X chromosomes
- 82 [6]. Dosage compensation requires orchestrating several gene-regulatory events across
- X chromosomes in hermaphrodites to decrease gene expression by half.
- 84 A core component of the dosage compensation machinery in *C. elegans* involves a
- 85 specialized condensin complex. Condensins are highly conserved protein complexes
- used in most cellular life, from prokaryotes to metazoans [7]. Condensin complexes are
- 87 characterized by their ring-shaped structure, and they hydrolyze ATP to extrude DNA
- 88 strands through the ring, thus leading to DNA coiling and loop formation [8]. This loop
- 89 extrusion activity is thought to be essential for chromosome compaction in mitosis and
- 90 meiosis [9]. Multicellular eukaryotes have two condensin complexes, condensin I and II,
- 91 functioning in mitosis and meiosis [10]. Similarly, C. elegans utilizes condensin I and II
- 92 complexes for chromosome compaction and segregation [11]. However, *C. elegans* has
- 93 a third condensin complex that specifically functions in dosage compensation of the X
- 94 chromosomes of hermaphrodites. The hermaphrodite-specific condensin is known as
- 95 condensin I^{DC} (Dosage Compensation) [11,12]. Condensins are composed of two
- 96 structural maintenance of chromosomes (SMC) proteins and three chromosome-
- 97 associated polypeptides (CAP) [13,14]. Condensin I^{DC} earns its name due to the four
- 98 shared protein subunits with condensin I. These subunits include the structural
- 99 maintenance of chromosomes (SMC) protein MIX-1 and the chromosome-associated
- polypeptides (CAPs) CAPG-1, DPY-26, and DPY-28. The difference between
- 101 condensin I^{DC} and condensin I is the second SMC subunit, DPY-27 in condensin I^{DC}
- and its paralog SMC-4 in condensin I [11,15,16]. Condensin I^{DC} compacts the dosage
- 103 compensated X chromosomes; thus, the X occupies less nuclear volume in

- hermaphrodites than in males [17,18]. At a higher resolution, condensin I^{DC} remodels
- the architecture of the X chromosomes to form topologically associating domains
- 106 (TADs) characterized by a higher frequency of *cis*-interactions within domains [19,20].
- Beyond condensin I^{DC}, the complete dosage compensation complex (DCC) in *C*.
- 108 elegans includes the proteins SDC-1, SDC-2, SDC-3, DPY-30, and DPY-21 [11,21–23].
- Together, these ten proteins bind and spread across the X chromosomes in
- 110 hermaphrodites, inhibiting RNA Pol II binding, thus lowering transcriptional output by
- half [24]. One of the non-condensin DCC subunits is DPY-21 [22]. It contains a Jumonji
- 112 C domain found in histone demethylases. DPY-21 has been shown to demethylate
- dimethylated histone 4 lysine 20 (H4K20me2) [25], previously deposited on histones by
- the activities of SET-1 and SET-4 [26,27], to the monomethylated form (H4K20me1).
- 115 Thus, by the X-specific demethylase activity of DPY-21, H4K20me1 is enriched on the X
- 116 chromosomes in hermaphrodites and contributes to further repression [25–27]. In
- addition to its demethylase function, DPY-21 has an additional uncharacterized role in
- dosage compensation [25,28]. Like other DCC members, DPY-21 activity is required to
- regulate the X chromosome effectively, as evidenced by the elevated X-linked gene
- expression in hermaphrodites with *dpy-21* mutations [25,29]. However, DPY-21 is not
- 121 necessary to recruit the other DCC members, and the loss of its function leads to mild
- defects in hermaphrodite *C. elegans* but no significant lethality [22].
- 123 Nuclear lamina interactions with heterochromatin provide an additional layer of gene
- regulation in *C. elegans*, impacting dosage compensation. In *C. elegans*,
- 125 heterochromatic regions of chromosomes are located near the nuclear periphery
- 126 [29,30]. Histone methyl transferases (HMTs) MET-2 and SET-25 target H3 lysine 9
- 127 (H3K9) on chromatin to deposit mono-, di-, and trimethylation [30]. The lamina-
- 128 associated protein CEC-4 binds to heterochromatic H3K9me regions on both the
- autosomes and the X [32]. The tethering of heterochromatic regions of the
- 130 chromosomes to the nuclear lamina contributes to stabilizing cell fates during *C*.
- 131 elegans development [32]. In addition, the loss of nuclear lamina tethering leads to the
- decompaction and relocation of the X into a more interior position in the nucleus and a
- 133 mild increase of X-linked gene expression without impacting autosomal gene
- expression, indicating dosage compensation defects [33]. Despite defects in the
- 135 chromosomal organization, mutants with non-functional CEC-4 survive with no apparent
- 136 phenotypes [32].
- Dosage compensation is set up in a stepwise manner over the course of development
- in *C. elegans*. The process is initiated around the 40-cell stage, when the DCC subunit
- 139 SDC-2 is expressed and localizes to hermaphrodite X chromosomes [34], which leads
- to the recruitment of the other DCC subunits [35]. This initiation step coincides with the
- loss of pluripotency of embryonic blastomeres [36,37]. DPY-21 localizes to the X after
- the initial loading of condensin IDC, and H4K20me1 becomes enriched on the X between
- the bean and comma stages of embryogenesis [25,36]. By the end of embryogenesis,
- most cells exit mitosis [38], after which the dosage-compensated state is maintained in

postmitotic cells. We refer to this stage as the maintenance phase. Earlier studies using cold-sensitive *dpy-27* alleles suggested that DPY-27 activity is essential during a critical developmental time window in mid-embryogenesis, after which loss of its function has a lesser impact on viability [39]. These results suggest that while condensin I^{DC} is required to initiate dosage compensation, other mechanisms may be responsible for maintaining dosage compensation, including ones mediated by DPY-21 and CEC-4.

The requirement for CEC-4 also changes with the differentiation state of embryonic cells. CEC-4 is required to tether heterochromatic transgenic arrays to the nuclear lamina in embryos but not in L1 larvae [32]. At the larval stages and beyond, additional mechanisms, including ones mediated by MRG-1 and CBP-1, contribute to sequestering heterochromatin to the nuclear lamina [40]. However, X chromosome compaction and nuclear lamina tethering are affected in *cec-4* adults, even in fully differentiated postmitotic cells [33]. We hypothesize that by sequestering the chromosome to the nuclear lamina, CEC-4 stabilizes the repression of the X chromosomes during the maintenance phase of dosage compensation.

In this study, we used the auxin-inducible degradation (AID) system to deplete the condensin I^{DC} subunit DPY-27 at various stages of development. We assessed the importance of condensin I^{DC} to X chromosome repression and organismal viability during the establishment and maintenance phases of dosage compensation. Our findings reveal that the continued presence of DPY-27 is required to maintain X chromosome repression after initial establishment. However, continued repression is less essential for viability during the maintenance phase. Additionally, we evaluated the hypothesis that the nuclear lamina protein CEC-4 helps stabilize the repressed state by combining *cec-4* mutations with depletion of DPY-27 or mutations in the histone demethylase *dpy-21*. We show that the loss of lamina associations resulting from mutations in *cec-4* exacerbates the defects caused by the lack of DPY-27 or DPY-21 function. Our results reveal the differential contributions of the various repressive pathways to X chromosome dosage compensation.

Results

175 The impact of DPY-27 depletion on hermaphrodite embryos

1	76	an	ıd	lar	va	e

- 177 Using a strain containing an auxin-inducible degron (AID)-tagged dpy-27 allele [41] and
- expressing the plant F-box protein TIR1 under a ubiquitous promoter (eft-3) [42]
- 179 (referred to as TIR1; dpy-27::AID, for complete genotype and allele information for all
- strains see the Materials and Methods), we were able to time the depletion of DPY-27
- by moving worms to auxin-containing plates during or after embryogenesis. To evaluate
- whether the lack of CEC-4 exacerbates the defects, we also generated a strain
- 183 containing the cec-4 (ok3124) mutation in addition to TIR1 and dpy-27::AID (referred to
- as TIR1; dpy-27::AID; cec-4). For controls, we used wild-type worms (N2), cec-4
- mutants, and a strain with AID-tagged *dpy-27* but no TIR1 expressing transgene
- 186 (referred to as *dpy-27::AID*).
- Our first experiment investigated the ability of embryos exposed to auxin to survive in
- the absence of DPY-27 throughout the entirety of embryonic development. To ensure
- that the maternally loaded DPY-27 is also depleted, we initiated our assay at the L4
- 190 larval stage of the parent before oocyte production begins (Fig 1A) [15]. L4 larvae were
- 191 placed on auxin-containing plates for a 24-hour egg-laying period, after which the
- parents were removed. This procedure ensures that both *in-utero* and *ex-utero*
- development occurs in the presence of auxin. Strains not exposed to auxin were mostly
- viable, although the *dpy-27::AID*-containing strains had a very low, but statistically
- significant, level of lethality (**Fig 1B**, Fisher's exact test, p values listed in **S1 File**). While
- auxin treatment did not significantly impact the survival of control embryos (N2, cec-4,
- 197 dpy-27::AID), 100% of TIR1; dpy-27::AID and TIR1; dpy-27::AID; cec-4 worms died as
- 198 embryos or L1 larvae (Fig 1B). These results indicate that DPY-27 function during
- 199 embryonic development is essential for the survival of hermaphrodite worms, which is
- 200 consistent with previous studies [39].

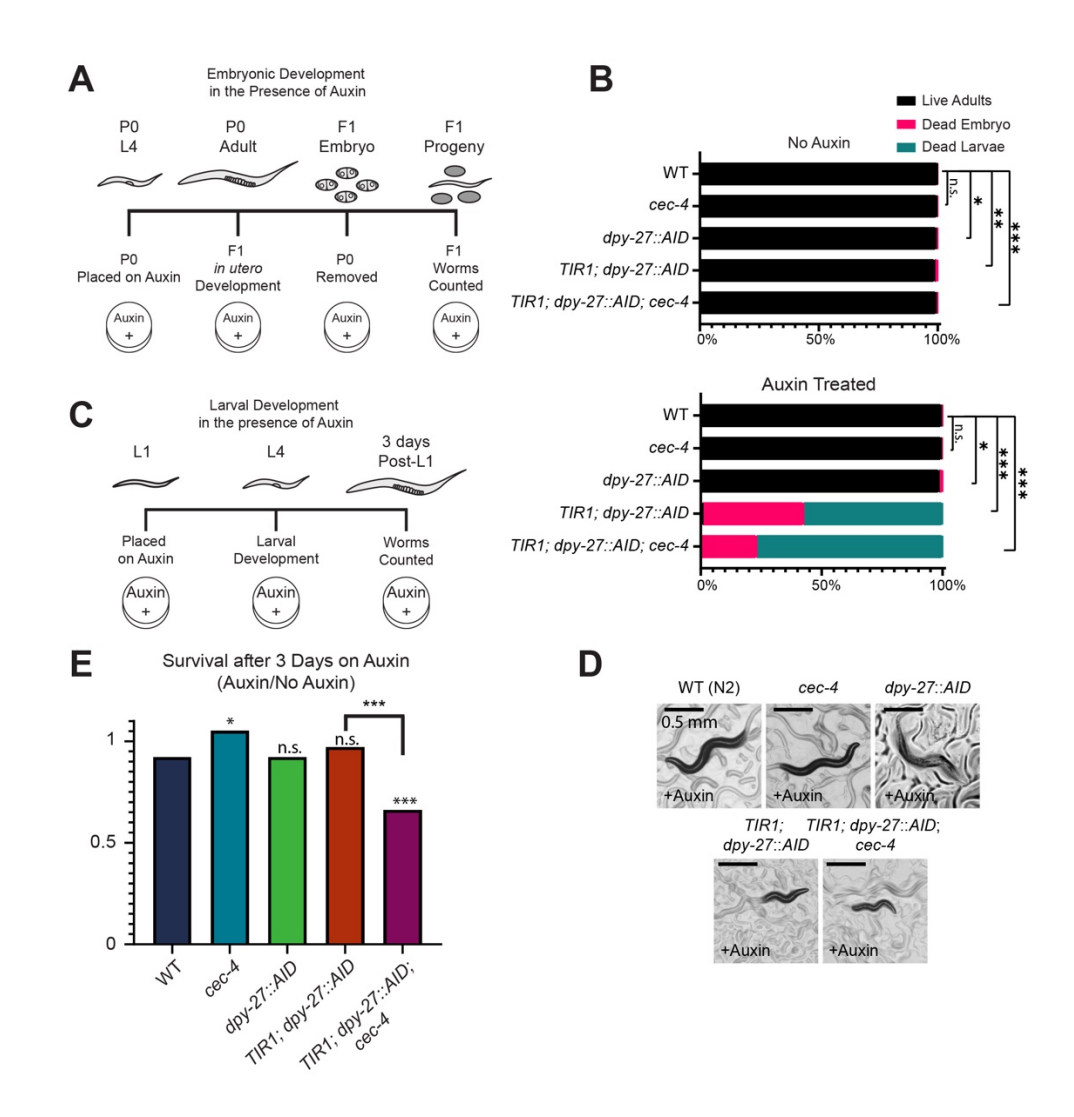


Fig 1. DPY-27 depletion leads to lethality and developmental defects. (A) Overview of the timeline of auxin exposure initiated from parental age L4 through F1 development. **(B)** Auxin exposure throughout embryogenesis results in compromised viability in TIR1; dpy-27::AID and TIR1; dpy-27::AID; cec-4 strains. Significance was determined by Fisher's exact test relative to wild-type values. Dead embryos and dead larvae were summed as one value for statistical analyses. Complete statistical analysis can be found in **S1 File**. **(C)** Overview of the timeline of auxin exposure from the L1 stage for three days. N2 worms in this time frame grow to young adults. **(D)** Phenotypic images of hermaphrodites exposed to auxin from the L1 stage for three days. Scale bar, 0.5 mm. **(E)** Larval survival on auxin relative to survival off auxin. Statistical significance was determined by Chi square tests. Complete statistical analyses can be found in **S2 File**. (n.s. = not significant, * = p < 0.05, ** = p<0.01, *** = p < 0.001).

At the onset of dosage compensation during early embryogenesis, condensin I^{DC} loads onto the X chromosomes in hermaphrodites [15]. However, it is unclear whether the sustained presence of the complex is essential once dosage compensation is

established. To assess the requirement for DPY-27 to remain on the X during larval development, we exposed our strains to auxin starting at the L1 larval stage for a period of three days. We compared survival on auxin-containing plates to survival on plates without auxin (Fig 1C). Strains developing without auxin exposure grew to adulthood and produced viable offspring in the timeframe of the experiment. In contrast to embryonic exposure, exposing larvae to auxin had a much lesser effect on survival. Most TIR1; dpy-27::AID larvae survived similarly to N2, cec-4, or dpy-27::AID controls (Fig 1E, Chi-square test, p values listed in S2 File). However, DPY-27 depleted strains developed slowly and exhibited developmental defects, including stunted growth (Fig. **1D)**. The rare embryo produced by these hermaphrodites did not hatch. Adding *cec-4* to the background lowered the survival rate, suggesting that lack of both DPY-27 and CEC-4 results in more severe defects than lack of DPY-27 alone (Fig 1E).

Exposure to auxin depletes DPY-27, disrupts DCC binding and H4K20me1 enrichment on the X

We next investigated the degree of DPY-27 depletion in auxin-treated strains relative to untreated. DPY-27 was visualized in each strain by immunofluorescence (IF) after worms were exposed to auxin for three days starting at the L1 larval stage. Due to the underdeveloped nature of the DPY-27 depleted strains, we based the timing of IF staining on the growth of wild type. After 3 days, wild-type N2 worms have developed into young adults. IF images were captured in intestinal nuclei. Intestinal cells are 32-ploid and their large size facilitates analyses of the nucleus. Before auxin treatment, all our strains had a wild-type pattern of DPY-27 localization within the nucleus of intestinal cells (Fig 2A), consistent with the lack of any visible defects or lethality in these strains. Auxin treatment in N2, cec-4, and dpy-27::AID strains led to no observable changes. However, in the TIR1-containing strains, TIR1; dpy-27::AID and TIR1; dpy-27::AID; cec-4, auxin treatment resulted in depletion of DPY-27 to background levels (Fig 2B), suggesting that auxin-induced degradation was successful.

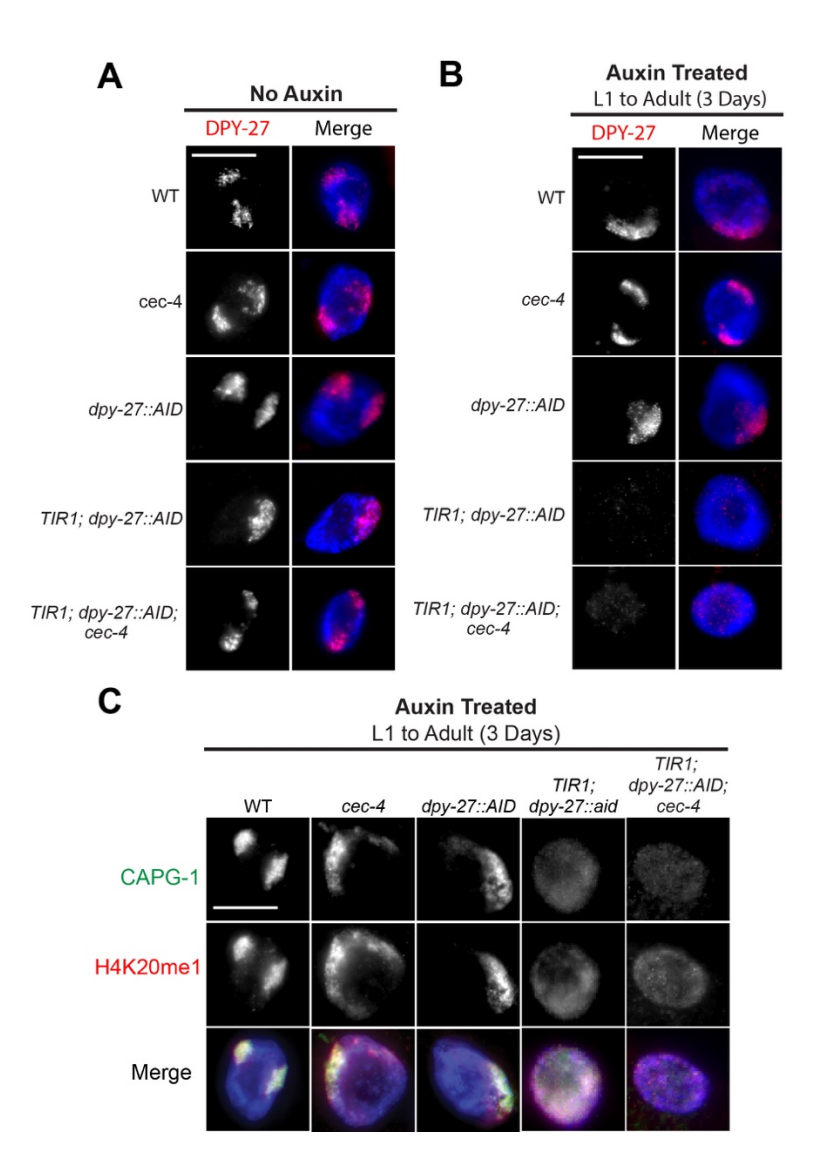


Fig 2. Auxin treatment leads to depletion of DPY-27, loss of DCC binding to the X, and disruption of the X-enrichment of H4K20me1. (A) Immunofluorescence staining of DPY-27 within the intestinal nuclei of young adult hermaphrodites is shown in the left columns, DAPI staining of DNA (blue) is merged with DPY-27 signal (red) in the columns to the right. DPY-27 is present within the nuclei in strains not exposed to auxin. (B) Exposure to auxin for 3 days starting at L1 results in a significant depletion of DPY-27 signal (red) by immunofluorescence in strains that contain *TIR1* and *dpy-27::AID* (C) DPY-27 depletion from L1 for three days leads to loss of CAPG-1 localization and H4K20me1 enrichment on the X. CAPG-1 (top row, green), H4K20me1 (middle row, red), and a merged image of all three channels, including DAPI DNA staining (bottom row, blue), are shown. (A-C) Scale bars, 10 μm.

The observation that *TIR1*; *dpy-27::AID* and *TIR1*; *dpy-27::AID*; *cec-4* larvae can survive despite complete or near complete depletion of DPY-27 prompted us to investigate the degree to which dosage compensation is maintained in these larvae. To assess the binding of other Condensin I^{DC} subunits to the X chromosome following DPY-27

- depletion, we performed IF staining for CAPG-1. In N2, *cec-4*, and *dpy-27::AID* strains, CAPG-1 maintains a signal pattern indicative of X chromosome binding. However, in *TIR1; dpy-27::AID* and *TIR1; dpy-27::AID; cec-4*, the CAPG-1 signal becomes non-specific and it diffuses throughout the entire nucleus (**Fig 2C**). Our results indicate that condensin I^{DC} no longer maintains localization to the X chromosomes following DPY-27 depletion.
- 267 We next assessed the enrichment of the histone modification H4K20me1 as a readout 268 for functional DCC binding. In wild-type N2 hermaphrodites, this histone modification is 269 specifically enriched on dosage-compensated X chromosomes [26,27], and this pattern 270 was maintained in cec-4 and dpy-27::AID strains. After exposure to auxin in TIR1: dpy-271 27::AID and TIR1; dpy-27::AID; cec-4 strains, H4K20me1 was no longer specifically 272 localized within the nucleus, resembling the pattern observed for CAPG-1 localization 273 with the IF signal spread throughout the entirety of the nucleus (Fig 2C). H4K20me1 274 first becomes enriched on dosage-compensated X chromosomes in mid-embryogenesis 275 [27,36], well before the L1 stage, when auxin treatment was initiated. We conclude that 276 the continued presence of DPY-27 and the DCC is required to maintain this chromatin 277 mark on the X chromosomes. The TIR1: dpy-27::AID and TIR1: dpy-27::AID: cec-4 278 strains appeared similar in this assay, suggesting that the presence or absence of CEC-279 4 does not contribute to the maintenance of the H4K20me1 mark.

The continued presence of DPY-27 is required to maintain X chromosome condensation and subnuclear localization

280

281282

283

284

285

286

287

288

289

290

291

292

293

294

295

296

297

298

299

300

301

The X chromosomes of wild-type hermaphrodites occupy a surprisingly low proportion of space in the nucleus compared to what is predicted based on DNA content [17]. We previously showed that in DCC mutants and in cec-4 mutant hermaphrodites, the X chromosomes decondense and relocate toward the more actively transcribed central region of the nucleus [33]. The DCC starts to compact the X chromosomes in early embryogenesis [17]. We tested if the continued presence of DPY-27 is necessary for maintaining the compact conformation and peripheral localization of the X. We performed whole chromosome X paint fluorescence in situ hybridization (FISH) to mark the X chromosome territories in intestinal nuclei. Without auxin treatment, the X chromosome signal appeared as expected: compact and near the nuclear periphery in all strains without a cec-4 mutation and more diffuse in strains with a cec-4 mutation (Fig 3A). After auxin treatment, the X chromosomes appeared enlarged in TIR1; dpy-27::AID as well (Fig 3B). We quantified these changes by measuring the proportion of nuclear volume occupied by the X chromosome (see Methods). The X chromosome occupied about 12-13% of the nuclear volume in wild type and close to 20% in cec-4 mutants (Fig 3C, S3 File for complete statistical analysis), which is consistent with previous results [33]. In the TIR1: dpy-27::AID strain, depletion of DPY-27 led to decondensation of the X chromosome to a degree similar to cec-4 mutants or to what was previously observed in worms treated with dpy-27 RNAi [17]. These findings demonstrate the critical role of DPY-27 in maintaining the compact conformation of the

X chromosome in wild-type hermaphrodites. In the *TIR1; dpy-27::AID; cec-4* strain, the X was already decondensed without auxin treatment due to the presence of the *cec-4* mutation, and depletion of DPY-27 led to a measurable level of additional decondensation (**Fig 3C**). These results indicate that the presence of DPY-27 maintains X compaction, and the additional loss off *cec-4* exacerbates decondensation.

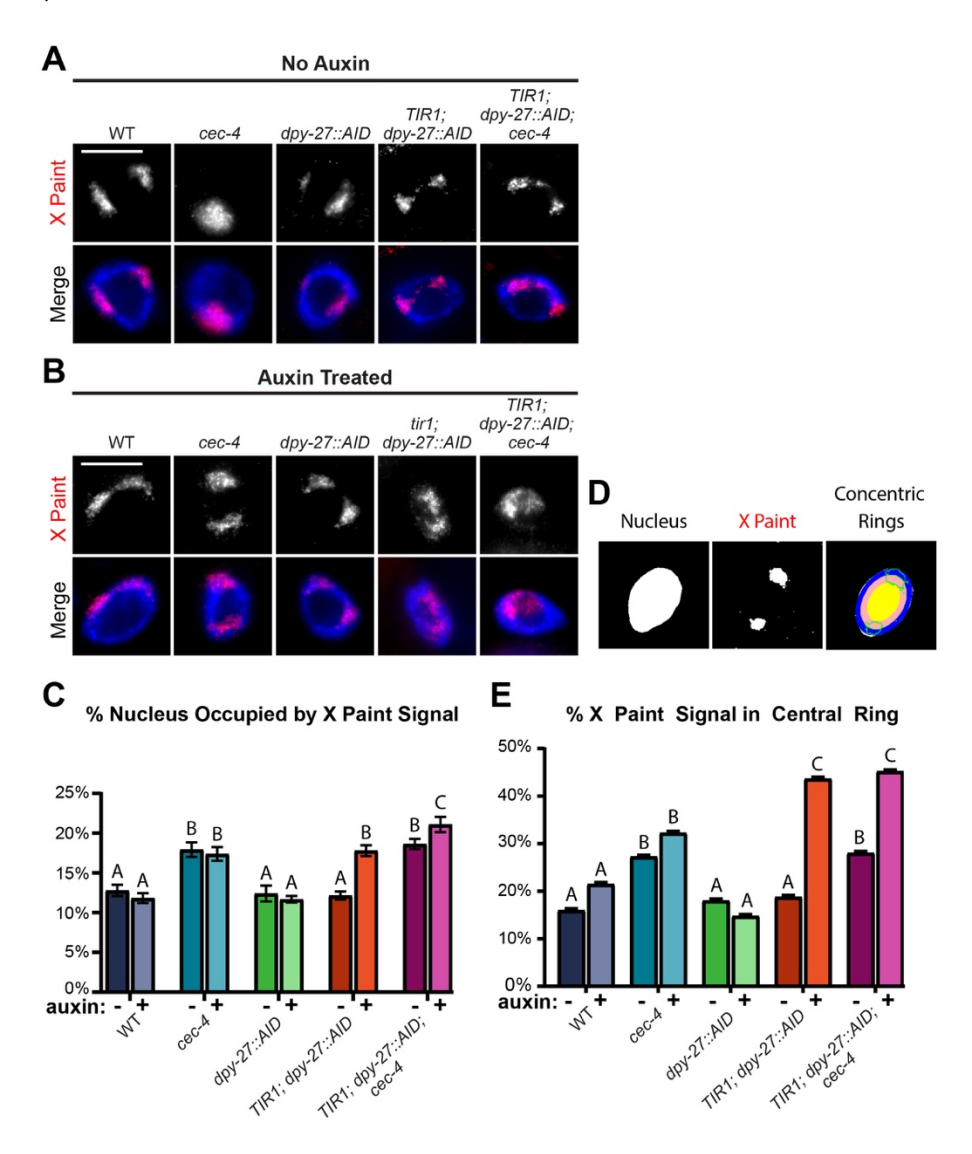


Fig. 3 The continued presence of DPY-27 is required for X compaction and peripheral localization within the nucleus. (A) Intestinal nuclei from adult hermaphrodites not exposed to auxin were stained with whole X chromosome paint FISH probe (top row, red), and DNA was labeled with DAPI (blue). Representative images are from young adult 3 days post-L1 hermaphrodites not exposed to auxin. **(B)** X chromosome paint FISH was performed in intestinal cells of hermaphrodites exposed to auxin from L1 for three days. **(C)** Quantifications of the X chromosome volume normalized to nuclear size (n = 20 nuclei). Hermaphrodites grown without auxin are indicated by "-", and auxin-treated worms are designated by "+". *dpy-27* depletion or *cec-4* mutation increases X decondensation. For complete statistical analysis see

S3 File. (D) Three-zone assay segmenting shown on a single slice from the middle of an intestinal nucleus. The amount of X signal (outlined in green) in each ring was quantified. **(E)** The proportion of the X paint signal seen in the central zone of the nucleus (n = 20 nuclei). Relocation to the center of the nucleus is increased DPY-27 depleted worms or *cec-4* mutants. Hermaphrodites grown without auxin are indicated by a "-" (bars on the left), and auxin-treated worms are designated by a "+". For complete statistical analysis see **S4 File. (A-B)** Scale bars, 10 μm. **(C, E)** Values sharing the same letter are considered statistically not different from each other (n.s. = p>0.05). Distinct letters indicate significant differences between the corresponding values (p<0.05, Student's t-test). Error bars indicate the standard error of the mean. Complete signal analyses in all concentric rings can be found in **Fig S1**.

Dosage compensation mechanisms makes the X chromosomes not only compact but also position the chromosomes near the nuclear periphery [33]. To assess any changes in subnuclear localization, we analyzed our X chromosome FISH signals in the various strains using a three-zone assay (see Methods) (Fig 3D). The localization of the X within the nucleus was assessed in three concentric zones, and the portion of the X signal in the central zone was quantified from a single focal plane taken from the middle of the nucleus. (Fig 3D). In wild-type hermaphrodites, we observed the expected X localization. Only a small portion of the signal reaches into the center ring, while the bulk of the X is located in the intermediate and peripheral zones of the nucleus (Fig 3E, S1 Fig, S4 File for complete statistical analysis), as observed before [33]. In cec-4 mutants (cec-4 and TIR1; dpy-27::AID; cec-4), significantly more of the X signal is in the center, as expected. The relocation is even more significant in DPY-27 depleted strains (Fig 3E). In both TIR1; dpy-27::AID and TIR1; dpy-27::AID; cec-4 strains, over 40% of the signal is localized in the central region, suggesting that the depletion of DPY-27 has a more significant impact on X nuclear localization than the cec-4 mutation. Adding cec-4 mutation did not significantly increase the degree of movement to the middle region compared to DPY-27 depletion alone. Overall, these data indicate that the continued presence of DPY-27 is required to maintain X compaction and peripheral localization and that adding a cec-4 mutation led to further X decompaction but no additional relocalization to the central zone of the nucleus.

The continued presence of DPY-27 is required in fully differentiated postmitotic cells

Thus far, we analyzed worms for which the auxin treatment began at the L1 larval stage and ended 3 days later (the duration of time in which N2 reaches adulthood). In this timeframe, intestinal nuclei undergo 4 rounds of endoreduplication and reach the stage of 32-ploidy [43]. To analyze the continued need for DPY-27 after these altered cell cycles have taken place and the cells have fully differentiated, we performed experiments where the auxin treatment began in adulthood (3 days past L1). The auxindegron system is very effective in *C. elegans*, with protein degradation observable within 30 minutes [42]. We subjected adult hermaphrodites to auxin for one hour to assess whether one hour was sufficient for DPY-27 degradation. In *TIR1*; *dpy-27::AID*

360

361

362 363

364

365

366

367 368

369

370 371

Fig 4. Rapid depletion of DPY-27 leads to a subsequent gradual loss of CAPG-1 and H4K20me1 enrichment on the X. (A) Young adult hermaphrodites were exposed to auxin for one hour before dissection, fixation, and IF staining for DPY-27 (red) and DNA (DAPI, blue). DPY-27 signal was significantly depleted in *TIR1; dpy-27::AID* and *TIR1; dpy-27::AID; cec-4* strains (B) Immunofluorescent analysis of young adult hermaphrodites using antibodies for CAPG-1 (green) and H4K20me1 (red) after auxin exposure for one hour (columns on the left) and 24 hours (columns on the right). (C) X paint FISH (red) staining of adult *TIR1; dpy-27::AID* and *TIR-1; dpy-27::AID; cec-4* after 24-hours of auxin exposure. (D) Quantification of the volume of the X paint FISH signal. Significance was determined by Student's t-test. Values sharing the same letter are not significantly different. Distinct letters indicate significant

373 differences between the corresponding values (p<0.05). WT data (\$) is repeated from Fig 3C. 374 Error bars indicate the standard error of the mean. (**A-D**) Scale bars, 10 μm.

375

376

377

378

379

380

381

382

383

384

385

386

387

388

389

390

391

392

393

394

395

396

397

398

399

400

401 402

403

404

405

406

407

408

409

410

411

412

413

Given the rapid depletion of DPY-27, we investigated potential alterations in mechanisms linked to dosage compensation. To assess whether H4K20me1 enrichment is sustained after DPY-27 loss, intestinal nuclei of young adult hermaphrodites exposed to auxin for one hour were stained with an antibodies targeting H4K20me1 and the DCC subunit CAPG-1. Auxin exposure for one hour resulted in the CAPG-1 signal appearing diffuse throughout the nucleus in TIR1; dpy-27::AID with and without cec-4, but with partial enrichment over a portion of the nucleus, presumably the X chromosome (Fig 4B, left). These results indicate that after DPY-27 depletion, the rest of the DCC also rapidly dissociates from the X, but with a slight delay compared to the DPY-27. Notably, H4K20me1 staining also appeared somewhat limited to this region but more diffuse than in controls. Strains in which DPY-27 was not depleted (cec-4 and dpy-27::AID) exhibited a clear overlap of the H4K20me1 and the CAPG-1 signals. comparable to no auxin controls. However, the changes in staining of H4K20me1 and CAPG-1 after one hour of auxin treatment are not as drastic as in hermaphrodites exposed to auxin for three days. To test whether prolonged exposure would lead to more complete loss of enrichment, we exposed young adult hermaphrodites to auxin for 24 hours. After 24 hours, TIR1; dpy-27::AID and TIR1; dpy-27::AID; cec-4 exhibited a complete loss of the X-enrichment of the CAPG-1 and H4K20me1 signals (Fig 4B, right), indistinguishable from results obtained with worms treated with auxin for three days of larval development (Fig 2C). We performed whole X paint FISH on strains exposed to auxin for 24 hours (Fig 4C). We observed X chromosome decondensation to levels similar to worms exposed to auxin for 3 days (Fig 4D). Hence, we conclude that the continued presence of DPY-27 is required to maintain the dosage-compensated state even in fully differentiated postmitotic cells and that depletion of DPY-27 leads to the rapid loss of features associated with dosage compensation.

X-linked genes are derepressed after DPY-27 depletion

We next tested whether these changes in X chromosome compaction, nuclear organization, and the depletion of repressive histone marks, led to increases in X chromosome gene expression in the *TIR1; dpy-27::AID* and *TIR1; dpy-27::AID; cec-4* strains when treated with auxin. Although nuclear organization and H4K20me1 enrichment were not significantly different with and without a mutation in *cec-4*, the reduced viability of auxin-treated *TIR1; dpy-27::AID; cec-4* larvae compared to *TIR1; dpy-27::AID* larvae also suggested that the X may be more derepressed in the strain also lacking *cec-4*. To test these hypotheses, we extracted total mRNA from synchronized L3 populations, which were grown in the presence of auxin starting at L1 or grown in the absence of auxin for controls. We performed these experiments at the L3 stage rather than at a later stage, because at this stage the delay in growth and development of the DPY-27 depleted strains is not yet apparent, and also to avoid

complications arising from the contributions from the germline where the X chromosomes are subject to regulation unrelated to dosage compensation [44]. At the L3 stage, the germline consists of only about ~60 cells, and thus the RNA extracted from whole worms represents predominantly somatic tissues [45]. The mRNA-seq readout is plotted as a log2-fold change in gene expression on autosomes and the X in auxin-treated samples compared to controls (Fig 5, Fig S2, S5 File).

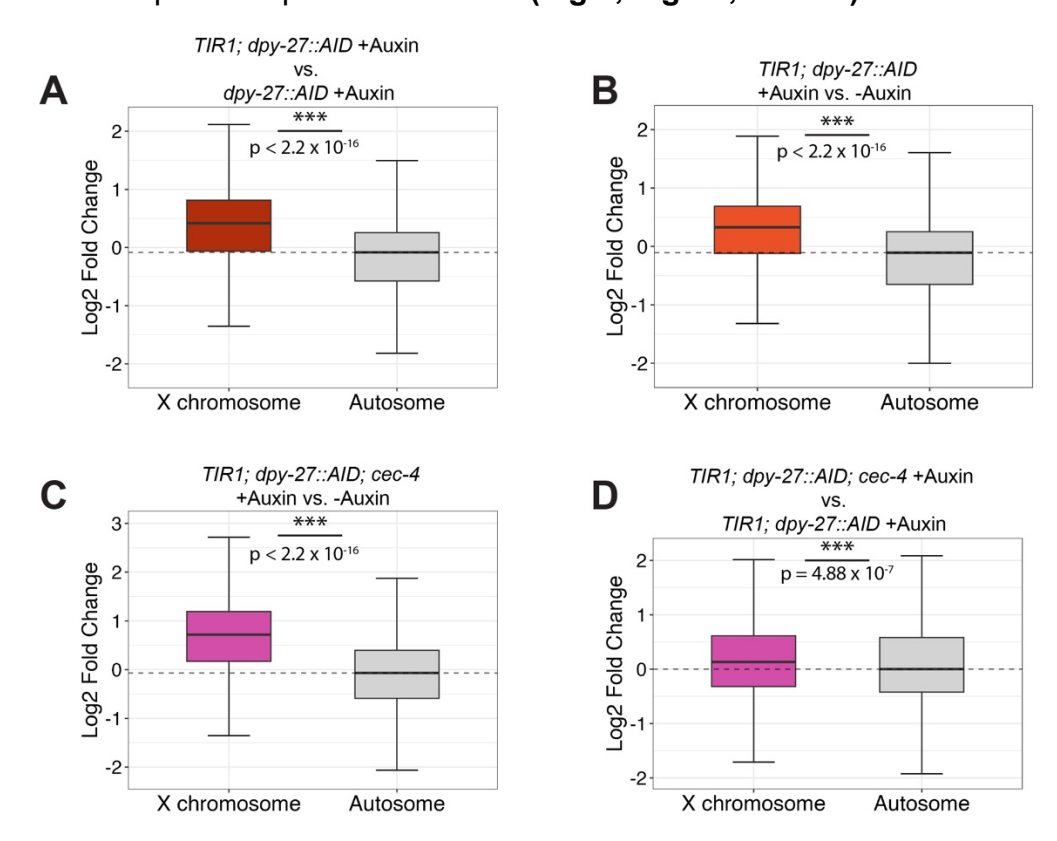


Fig 5. The X-linked gene expression is derepressed in strains depleted of DPY-27. (A-D) Boxplots depicting the distribution of the log2 fold change of the X-linked genes and of the autosomal genes in strains being compared. A Wilcoxon rank-sum test was used to determine the statistical significance of the differential gene expression between the X and autosomes. (n.s. = not significant, * = p < 0.05, ** = p<0.01, *** = p < 0.001) (A) The log2 fold change in gene expression of the autosomes and the X chromosomes of TIR1; dpy-27::AID relative to the dpy-27::AID after both strains were exposed to auxin. (B) TIR1; dpy-27::AID treated with auxin compared to the same genotype grown in the absence of auxin. (C) TIR1; dpy-27::AID; cec-4 treated with auxin was compared to no auxin treatment. (D) TIR1; dpy-27::AID; cec-4 compared to TIR1; dpy-27::AID, both treated with auxin.

Without exposure to auxin, the *dpy-27::AID* strain had similar gene expression levels to N2, although the slight X derepression was statistically significant. The minimal change in gene expression suggests that tagging DPY-27 with the degron tag did not significantly disrupt its function (**Fig S2A**). *cec-4* strains treated with auxin also displayed slight X depression compared to *cec-4* mutants without auxin exposure,

437 indicating a minimal influence of auxin treatment on gene expression regulation (Fig 438 **S2B)**. The TIR1; dpy-27::AID and the TIR1; dpy-27::AID; cec-4 strains also had a small 439 degree of X derepression compared to wild type even in the absence of auxin, possibly 440 due to somewhat leaky TIR1 activity (Fig S2C and D), which is a phenomenon noted by 441 other research groups as well [46-48]. Therefore, to assess the increase in X-linked 442 gene expression resulting the loss of DPY-27, we compared gene expression levels in 443 the same strain with and without auxin and/or in auxin-treated strains with and without 444 TIR1 expression (Fig 5). In comparison to dpy-27::AID, the strain TIR1; dpy-27::AID had 445 significant upregulation of the X chromosome when treated with auxin, while autosomal 446 gene expression remained unchanged (X derepression (defined as median X-linked 447 log2 fold change – median autosomal log2 fold change) = 0.503) (Fig 5A). Similarly, 448 auxin-treated TIR1: dpy-27::AID exhibited significant X derepression (0.435) compared 449 to non-auxin-treated (Fig 5B). These results demonstrate that depletion of DPY-27 450 during the maintenance phase of dosage compensation leads to significant X 451 derepression.

452 We then investigated whether the absence of CEC-4 further enhanced X derepression. 453 Comparing the mRNA-seg gene expression profiles of TIR1: dpy-27::AID: cec-4 treated 454 with auxin to untreated populations of the same genotype, we observed a significant 455 increase in X-linked gene expression (0.78) (Fig 5C). The degree of X derepression 456 was greater than that caused by auxin treatment in TIR1; dpy-27::AID without the cec-4 457 mutation. These results suggest that the loss of cec-4 may exacerbate X dosage 458 compensation defects. To confirm, we compared TIR1; dpy-27::AID; cec-4 to TIR1; dpy-459 27::AID after auxin treatment. The difference between these two populations was 460 substantial (0.13), suggesting that depletion of DPY-27 leads to a greater level of X 461 derepression in a strain that lacks CEC-4 (Fig 5D). These results are consistent with 462 CEC-4 playing a supporting role in helping to maintain stable X chromosome repression 463 in differentiated cells.

Loss of *cec-4* activity exacerbates dosage compensation defects caused by a mutation in *dpy-21*

464

465

466 Our experiments showed that the loss of CEC-4 sensitizes hermaphrodite *C. elegans* to 467 dosage compensation defects caused by DPY-27 depletion (Fig 5D). To test whether 468 loss of CEC-4 also exacerbates defects caused by other dosage compensation 469 mutations, we sought to understand the interplay between CEC-4, known for its role in 470 tethering the X chromosomes to the nuclear lamina [33], and DPY-21, whose activity 471 leads to X-specific enrichment of H4K20me1 [25]. Individually, the mutations in these 472 pathways lead to phenotypes related to dosage compensation defects and changes in 473 X-linked gene expression, but despite these changes, the mutants are viable 474 [22,25,26,32,33]. Since dpy-21 null mutants (dpy-21(e428)) are viable [22], we 475 performed these experiments with the null mutant rather than using the AID system. 476 Therefore, our experiment tested the impact of these mutations throughout the lifespan 477 of the animals, including both the establishment and the maintenance phases of dosage compensation. We constructed a double mutant *cec-4* (*ok3124*) IV; *dpy-21*(*e428*) V strain (referred to as *cec-4*; *dpy-21*). The strain is viable but with visible defects, such as a Dpy phenotype.

We first evaluated the ability of hermaphrodites lacking functional *cec-4* and *dpy-21* to lay viable eggs. The total number of eggs laid by *cec-4*; *dpy-21* hermaphrodites was significantly smaller than all other strains observed, including the *dpy-21* and *cec-4* single mutants (**Fig 6A**). In all strains, most embryos hatched into larvae within 24 hours (**Fig 6B**). Most wild-type (N2) and *cec-4* mutant larvae developed into adulthood. While the viability of *dpy-21* mutant larvae was somewhat reduced, it was not significantly different from the viability of *cec-4*; *dpy-21* double mutants (**Fig 6C**). Overall, these results suggest that the addition of the *cec-4* mutation does decrease the overall fitness of *dpy-21* mutants.

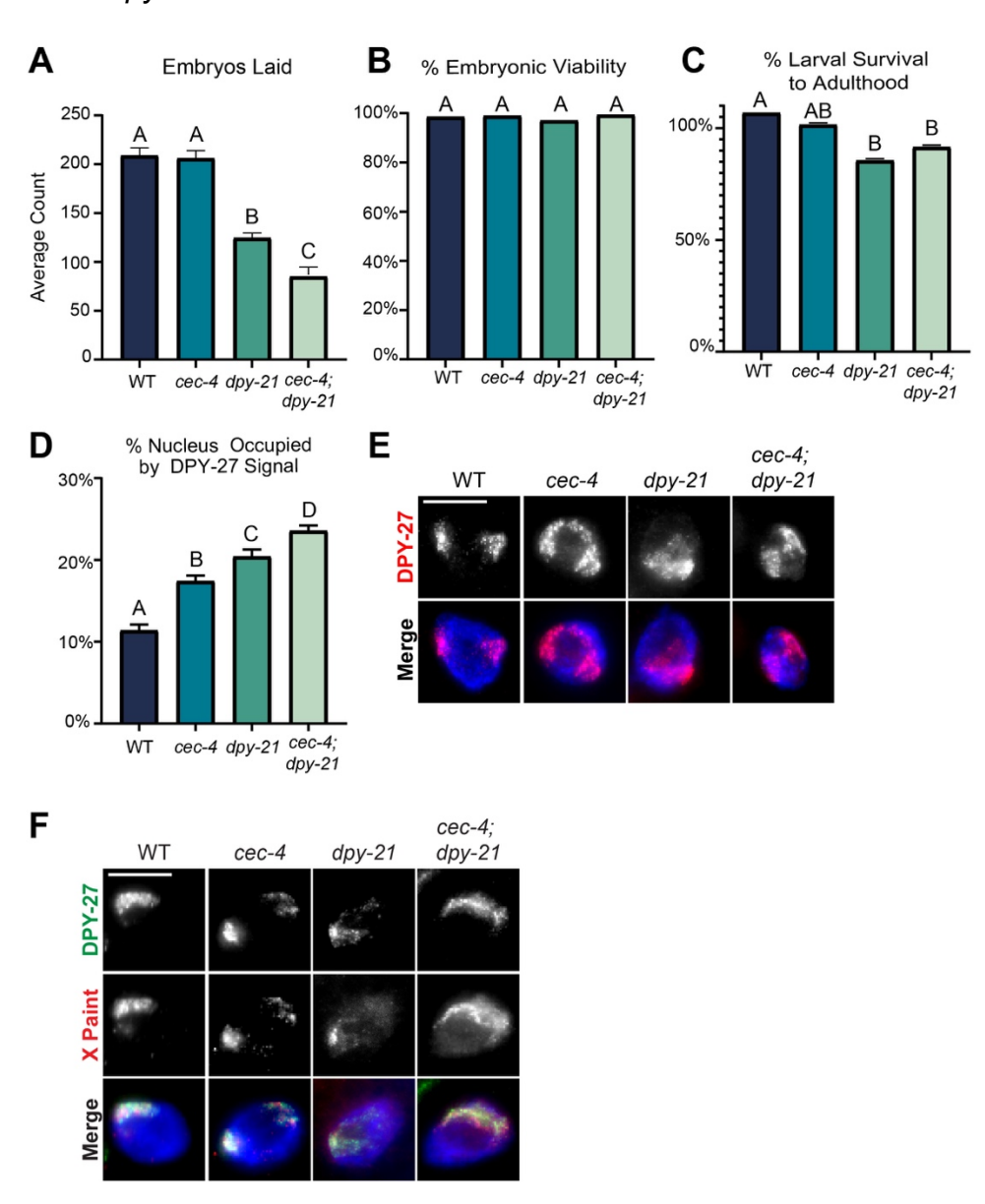


Fig 6. Loss of CEC-4 exacerbates dosage phenotypes caused by mutations in dpy-21.(A) The average of total number of eggs laid. A mutation in *dpy-21* decreases the average brood size. The double mutant, *cec-4; dpy-21*, yields the smallest brood. (B) The average percentage of embryos that hatched after 24 hours (hatched embryo after 24 hours/total embryo). (C) The average percentage of larvae that survived to adulthood. The few embryos laid by the *cec-4; dpy-21* strain can survive to adulthood but at a frequency lower than that of the wild type. (A-C) The error is reported as the standard error of the mean (n = 6-8 hermaphrodites). For statistical analysis see S6 File. (D) The extent of X chromosome decompaction. Error bars represent standard error of mean (n = 20). For statistical analysis, see S7 file. (E) Representative images of adult hermaphrodite intestinal nuclei stained for DPY-27 (top, red) and DNA (bottom, DAPI, blue). (F) DPY-27 (green) co-localizes to the X paint FISH signal (red) in all assayed strains. (E, F) Scale bar, 10 μm. (A-D) Values sharing the same letter are considered not statistically significantly different (n.s. = p>0.05). Distinct letters indicate significant differences between the corresponding values (p<0.05, Student's t-test).

We employed DPY-27 staining to mark the X chromosomes to assess the level of X chromosome compaction. All mutants exhibited a prominently decondensed X chromosome (**Fig 6E**). Further quantitative analysis revealed that the X chromosomes were decondensed in *cec-4* and *dpy-21* single mutants, but in the *cec-4*; *dpy-21* double mutant strain the X occupied an even more significant proportion of the nucleus (**Fig 6D**). The localization of DPY-27 to the X chromosome was not influenced by the loss of *cec-4* and/or *dpy-21* (**Fig 6F**). These observations show that adding the *cec-4* mutation to *dpy-21* mutants augments some defects associated with dosage compensation.

To determine the impact of these mutations on X chromosome gene repression, mRNAseg was performed in L3 hermaphrodites (Fig S3, See S5 File for statistical analysis). We previously reported subtle upregulation of the X chromosomes in cec-4 mutant L1 larvae compared to the wild type [33]. In L3 larvae, this upregulation was even more modest and not statistically significant (X derepression = 0.027, p = 0.421) (Fig 7A), suggesting that lack of CEC-4 alone does not have a significant impact on X-linked gene regulation despite the observed changes in X chromosome compaction and nuclear localization. In contrast, the dpy-21 mutant displayed a more pronounced derepression of the X chromosome (0.612, p < 2.2×10^{-16}) (Fig 7B), consistent with previous results [25,29]. When we compared the cec-4; dpy-21 double mutant to the wild type, we observed an even more drastic change in gene expression (X depression = 0.721, p = 2.2×10^{-16}) (Fig 7C). Furthermore, when juxtaposing the cec-4: dpy-21 double mutant against its single mutant counterparts, the results underscored that cec-4; dpy-21 expressed X-linked genes at a higher level than either single mutant (cec-4; dpy-21 vs cec-4: X derepression = 0.669, p = 2.2 x 10⁻¹⁶, and cec-4; dpy-21 vs dpy-21: X derepression = 0.09, p = 5.05×10^{-13}) (Fig 7D and E). Given the relatively minor derepression of the X chromosome in cec-4 mutants, a significant increase in the Xlinked gene expression levels of cec-4; dpy-21 compared to cec-4 alone was expected (Fig 7D). The *dpy-21* single mutant already exhibited an upregulation in X chromosome gene expression; however, the cec-4; dpy-21 double mutant significantly surpassed it in X derepression (Fig 7E). While cec-4, as a single mutation, does not substantially

impact X-linked gene expression, our results show that the loss of *cec-4* sensitizes hermaphrodites to additional dosage compensation defects.

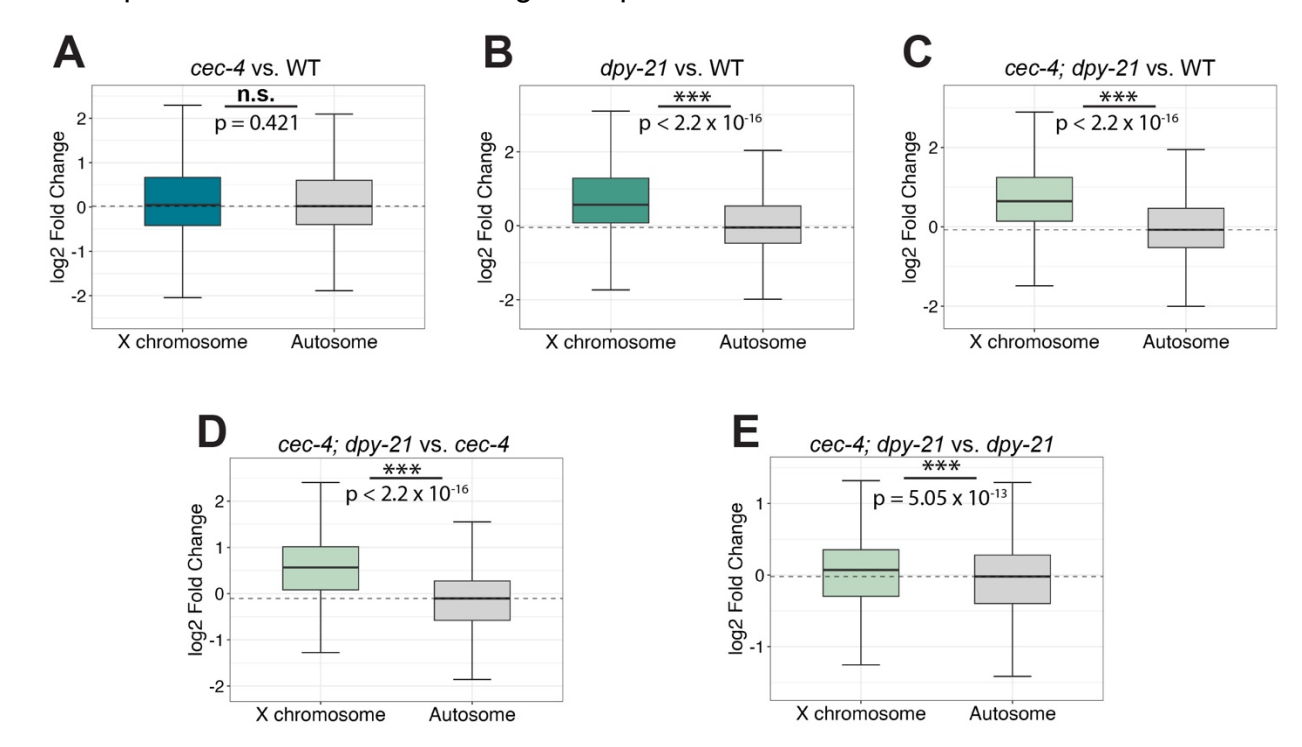


Fig 7. Loss of CEC-4 exacerbates gene expression defects caused by mutations in *dpy-21.* (A-E) Boxplots depicting the distribution of the expression of X-linked genes and expression of genes on autosomes. Gene expression is plotted as the log2 fold change of the strains being compared. Statistical significance is determined by the differences in gene expression between the X and autosomes by a Wilcoxon rank-sum test. (n.s. = not significant, * = p < 0.05, ** = p<0.01, *** = p < 0.001) (A) The log2 fold change in gene expression of the autosomes and the X chromosomes in *cec-4* mutant relative to the wild type (N2). (B) The log2 fold change in gene expression of the autosomes and the X chromosomes in *dpy-21* mutants relative to wild type (N2). (C) The log2 fold change in gene expression in *cec-4*; *dpy-21* compared to *cec-4*. (E) The log2 fold change in gene expression in *cec-4*; *dpy-21* compared to *dpy-21*. The derepression of the X chromosome genes is significantly higher in the double mutant than in single mutants.

Discussion

In this study, we investigated the relative contributions of the DCC to two phases of dosage compensation: establishment and maintenance. We depleted DPY-27, a core protein subunit of the dosage compensation machinery, condensin I^{DC}, using the auxininducible degron system during embryonic and larval development. Our data indicated that DPY-27 function is essential during embryonic development, but the protein is dispensable for hermaphrodite survival during larval and adult stages. In an additional dosage compensation mechanism, the non-condensin DCC member DPY-21 significantly contributes to X-linked gene repression by enriching H4K20me1 on the X chromosome [25]. We show that the enrichment of H4K20me1 is lost rapidly after DPY-27 depletion, indicating that the mark must be continuously maintained, presumably by

- DPY-21 recruited to the X by DPY-27. In addition, DPY-27 depletion leads to X
- 562 chromosome decondensation and relocation to a more central position in the nucleus,
- as well as significant increases in X-linked gene expression. In addition to the
- 564 contributions of the DCC, nuclear lamina association of the X chromosome via
- 565 H3K9me3 binding to CEC-4 also contributes to X morphology and repression [33]. We
- 566 found that a loss-of-function mutation in cec-4 amplifies the sensitivity of
- hermaphrodites to the depletion/mutation of other dosage compensation processes.
- 568 These results suggest that nuclear lamina anchoring by CEC-4 serves to stabilize
- repression initiated by condensin I^{DC} or H4K20me1. By loss-of-function mutations in
- 570 cec-4 and dpy-21 and depletion of DPY-27, we unexpectedly revealed that larval and
- adult hermaphrodites are resilient to depletion of known dosage compensation
- 572 mechanisms and substantial increase in X-linked gene expression.

Condensin I^{DC} function is required for embryonic viability but not for larval and adult viability

- 575 A previous study using a cold-sensitive mutant for *dpy-27* demonstrated that inactivating
- 576 DPY-27 during the comma stage of embryonic development leads to more extensive
- 577 lethality than inactivation of the protein at later stages. However, the differences in
- viability counts at the different temperatures were only about 20% [39]. We re-examined
- 579 this question using the auxin-mediated degradation system, where adding auxin leads
- 580 to rapid and near complete depletion of DPY-27. Prior to auxin treatment, the strains
- had essentially 100% viability, while auxin treatment during embryogenesis led to
- essentially 100% lethality. These results demonstrate that condensin I^{DC} activity is
- 583 essential during embryonic development when cell fates are being specified, and cells
- begin to differentiate into different cell types. At the end of embryonic development, the
- 585 embryo consists of about 500 cells, the majority of which have exited the cell cycle and
- begun terminal differentiation [38]. Depletion of condensin I after embryogenesis is not
- 587 incompatible with viability despite developmental abnormalities in depleted larvae. This
- incompatible with viability despite developmental abnormalities in depicted fairvae.
- result raised two possibilities. First, it is possible that dosage compensation, once
- established, can be maintained in the absence of condensin I^{DC}. Second, it is possible
- 590 that X chromosome repression is not maintained but the larvae can tolerate defects in
- 591 X-linked gene regulation. Our results, discussed below, are consistent with the second
- 592 scenario.

593 594

573574

Condensin I^{DC} must remain on the X to maintain the condensed conformation

- We show that compaction of the dosage compensated X cannot be maintained without
- 596 DPY-27. By varying durations of auxin exposure and observing the condensin I^{DC}
- 597 subunit CAPG-1, we saw the gradual loss of of condensin I^{DC} enrichment on the X (Figs
- 598 2 and 4). We propose that the absence of DPY-27 leads to the destabilization of the
- 599 condensin I^{DC} ring, resulting in the eventual release of the complex from the X. The X
- 600 chromosome also decondenses after condensin I^{DC} loss, indicating that chromosome
- 601 compaction must be actively maintained. Previous research investigating the

maintenance of mitotic or meiotic chromosome architecture demonstrated that depletion or inactivation of mitotic condensin subunits after chromosome condensation has taken place leads to disorganized chromosome structure with reduced rigidity or a larger surface area [49-52]. Similar to what we observed about the continued need for condensin IDC to maintain the compact structure of dosage compensated X chromosomes, maintenance of mitotic chromosome architecture also requires the continued presence of condensin. However, in the studies of mitotic chromosomes, compaction was maintained after condensin loss, only the organization or rigidity of chromosomes was altered. In our study, the interphase X chromosome was was not maintained. It has been suggested that during mitosis additional mechanisms, such as posttranslational histone modifications, contribute to chromosomes condensation [53]. We hypothesize that in the absence of these mitosis-specific histone modifications in interphase, condensin function is necessary for compaction. We note that two posttranslational histone modifications associated with mitosis, namely enrichment of H4K20me1 and depletion of H4K16ac, are also features of interphase dosage compensated X chromosomes of C. elegans [26,27,53–55]. However, additional mitotic histone modifications that are not present on dosage compensated X chromosomes (for example H3S10Ph or depletion of additional acetylation marks) may also contribute to condensin independent chromosome compaction in mitosis [56]. Our findings indicate that the complete condensin complex must remain associated with the X for the maintenance of compaction during developmental stages in which most cells are post-mitotic. It will be interesting to investigate the maintenance of chromosome architecture changes on dosage compensated Xs at higher resolution, such as formation of TADs using Hi-C.

The presence of DPY-27 is required to actively maintain the enrichment of H4K20me1 on the X

Concurrently with the loss of CAPG-1 signal, the H4K20me1 mark exhibits a loss of specific localization on the X with increasing auxin exposure time (Figs 2 and 4). We propose that the continued presence of DPY-21 (presumable recruited by DPY-27) on the X is necessary to maintain H4K20me1 enrichment on the X. Notably, the presence of DPY-21 is not essential for the localization of condensin I^{DC} on the X; however, for DPY-21 to bind the X, the presence of condensin I^{DC} is required [22]. Our results are similar to what was seen for H3K9me2 and MET-2. Maintenance of this chromatin mark in *C. elegans* also requires the continued presence of the enzyme that places it [57]. Our results suggest that functional Condensin I^{DC} plays a role in maintaining the localization of DPY-21 on the X, and its continued presence is required even in post-mitotic developmental stages. We hypothesize that in the absence of DPY-27 and DPY-21, either there is frequent enough histone turnover to lose the H4K20me1 enrichment or that the X is rendered accessible to histone modifiers that remove the H4K20me1 or modify the mark to di- or trimethylation.

Condensin I^{DC} is required to maintain X-linked gene repression in hermaphrodites

642643

644

645

646

647

648

649

650

651

652

653

654

655

656

657

658

659

660

661

662

663

664

665

666

667 668

669

670

671

672

673

674

675

676

677

678

679

680

Severe depletion or mutation of dosage compensation in *C. elegans* is hermaphrodite lethal. Unexpectedly, we observed that hermaphrodites survive as larvae with severe depletion of DPY-27, albeit with major phenotypic defects (Fig 1C). Furthermore, they survive without other vital contributors to X-linked gene regulation in addition to DPY-27 depletion, namely, nuclear lamina tethering by CEC-4 and H4K20me1 (Fig 2C). In short, auxin-treated TIR1: dpy-27::aid: cec-4 larvae survive without measurable activity of any known dosage compensation mechanism. Our study revealed increases in Xlinked gene expression beyond levels reported in dpy-27 null mutant embryos or L1 larvae (log2 fold change in X-linked gene expression of less than 0.3) [29] or sdc-2 mutant embryos treated with sdc-2 RNAi (log2 fold change about 0.6) [58]. Dosage compensation defects in these mutants lead to lethality. Our most significant increase in X-linked gene expression was measured in TIR1; dpy-27::AID; cec-4 L3 larvae after auxin exposure with a log2 fold change in X-linked gene expression at a value of 0.78 (Fig 5). These larvae survive despite more significant gene expression defects than previously reported for embryos dying of dosage compensation defects. We suggest that the absence of these dosage compensation processes is acceptable in these animals because the continued repression of the X is no longer essential after early development once cell fates have been specified and the cells have differentiated.

In mice, the critical contributor to dosage compensation, the long non-coding RNA Xist, can be deleted with minimal change to X repression as long as it is deleted during the maintenance phase after X chromosome inactivation is fully established [59,60]. However, unlike the continued repression of the mouse X despite the loss of Xist, we observed a significant derepression of X-linked genes in C. elegans hermaphrodites after the depletion of DPY-27. The difference might be due to the nature of the repressive mechanisms. In mice, X chromosome inactivation involves the establishment of facultative heterochromatin on the X chromosomes, including DNA methylation and heterochromatic histone modifications [61]. Studies in other organisms have shown that these chromatin marks can be maintained by propagating them during the S phase [62– 65], even without the initial trigger. The repressive mechanisms involved in *C. elegans* dosage compensation are different. H4K20me1 patterns are not propagated during DNA replication; in fact, H4K20me1 levels decrease in S phase due to the activity of an H4K20me1 demethylase PHF8 [66]. Instead, H4K20me1 is thought to be established during mitosis [54] and then converted to H4K20me2/3 methylation after mitotic exit [54]. Our results suggest that maintenance of this mark on dosage compensated X chromosomes requires the continued presence of DPY-27, presumably recruiting the H4K20me2 demethylase DPY-21 [25].

The loss of function of cec-4 sensitizes hermaphrodites to the loss of DPY-27 or DPY-21

683 The cec-4 mutation, combined with DPY-27 depletion, showed only minor changes in 684 nuclear compartmentalization and chromosome compaction compared to DPY-27-685 depleted strains with functional CEC-4 (Figs 3 and 4). However, there was a notable 686 decrease in hermaphrodite viability of DPY-27 depleted larvae with a cec-4 mutation 687 compared DPY-27 depleted larvae without a cec-4 mutation (Fig 1E), suggesting 688 disruption to X-linked gene regulation approaching unacceptable limits for survival. 689 When a cec-4 mutation was combined with a dpy-21 mutation, there was an observable 690 increase in X decompaction and a decrease in brood size in the double mutant 691 compared to single mutants, again suggesting greater disruption to dosage 692 compensation (Fig 6). mRNA-seg analysis indicated that the loss-of-function mutation 693 of cec-4 alone minimally increased X-linked gene expression (Fig 7A). However, in 694 scenarios where a cec-4 mutation was coupled with DPY-27 depletion or dpy-21 695 mutation, we observed a substantial increase in X-linked gene expression, significantly 696 more than in strains without the *cec-4* mutation (Figs 5, and 7). Previous studies have 697 highlighted the involvement of CEC-4 in cellular differentiation and stabilizing cell fates 698 [32]. Cells actively undergoing differentiation demand precise gene expression levels. 699 However, we hypothesize that the loss of some repressive mechanisms after 700 differentiation are acceptable, partly because CEC-4 may help lock down established 701 gene expression patterns, including the repressed state of dosage-compensated X 702 chromosomes. It should be noted, however, that the loss of cec-4 challenges the health 703 of C. elegans larvae depleted of other dosage compensation proteins, but most of the 704 larvae survive. We hypothesize that losing these mechanisms, including CEC-4 705 function, at the larval developmental stage does not result in outright lethality because 706 cellular differentiation is more complete.

- 707 While DCC-mediated mechanisms are crucial for viability during the establishment of
- dosage compensation, our results demonstrate that they are not essential for survival during the maintenance stage. During larval and adult developmental stages,
- 710 hermaphrodites survive without any known dosage compensation activity. This
- 711 resilience raises questions about the necessity of continued X repression after
- 712 embryonic development.

713

Acknowledgments

- 714 We thank Sarah VanDiepenbos, Hend Almunaidi, and Lillian Tushman for their
- 715 contributions to a preliminary analysis of the cec-4 and dpy-21 mutants, as well as all
- 716 members of the laboratory for helpful discussions. We would like to thank the laboratory
- of Dr. JoAnne Engebrecht for sharing the JEL1197 strain [41].

Materials and Methods

Caenorhabditis elegans Strains

The strains used are shown in the table below. Strains were maintained at 20°C on nematode growth media (NGM) plates seeded with the *Escherichia coli* strain OP50 as a food source, as described in [67]. For some experiments requiring larger number of worms, strains were grown on high-growth media (HGM) plates were seeded with *E. coli* strain NA22, as described in [68].

Genotype	Strain	Source
Wild Type	Bristol N2	CGC
dpy-21(e428) V	EKM71	This study
cec-4 (ok3124) IV	EKM121	This study
cec-4 (ok3124) IV; dpy-21(e428) V	EKM222	This study
ieSi57[Peft-3::TIR1::mRuby::unc-54 3'UTR,	EKM237	This study
cb-unc-119(+)] II; dpy-27::AID::MYC		
(xoe41) III		
dpy-27::AID::MYC (xoe41) III	EKM227	[41]
dpy-27::AID::MYC (xoe41) III; cec-4	EKM233	This study
(ok3124) IV		
ieSi57[Peft-3::TIR1::mRuby::unc-54 3'UTR,	EKM238	This study
cb-unc-119(+)] II; dpy-		
27::AID::MYC(xoe41) III; cec-4(ok3124) IV		
wrdSi3 [sun-	JEL1197	[41]
1p::TIR1::F2A::mTagBFP2::AID*::NLS::tbb-		
2 3'UTR] II; dpy-27(xoe41[dpy-		
27::AID::myc]) III; him-8 (me4) IV		
unc-119 (ed3); ieSi57 [Peft-	CA1200	[42]
3::TIR1::mRuby::unc-54 3'UTR, cb-unc-		
119(+)]		

725

718

- 726 The alleles for dpy-21 (e428) and cec-4 (ok3124) were initially acquired from the
- 727 Caenorhabditis Genetics Center (CGC) as the strains CB428 and RB2301, respectively.
- 728 Each strain was backcrossed to Bristol N2 six times to generate the strains EKM71 dpy-
- 729 21 (e428) and EKM121 cec-4 (ok3124). EKM222 was obtained by crossing EKM71 to
- 730 EKM121.
- 731 The strain JEL1197 was received from and generated by [41]. To isolate the dpy-
- 732 27::AID::MYC (xoe41) allele, JEL1197 was crossed to wild type to produce EKM227.
- 733 EKM227 was then crossed to CA1200 [42] to create EKM237.
- 734 To add cec-4 (ok3124) to the background, EKM227 was crossed with EKM121. The
- subsequent strain, EKM233, was crossed with CA1200 to generate EKM238.

736 **Antibodies**

740

754

755

- 737 Antibodies used in this study include rabbit anti-H4K20me1 (Abcam ab9051), rabbit
- anti-DPY-27 [11], and goat anti-CAPG-1 [33]. Secondary antibodies for anti-goat and
- anti-rabbit were purchased from Jackson Immunoresearch.

Synchronized worm growth and collection

- 741 To obtain synchronized worm populations, gravid adults were bleached to collect
- embryos [69]. During bleaching, the hermaphrodites degrade and leave only embryos,
- which are then collected. After washing with sterile 1X M9 salt solution [70], the
- 744 embryos are isolated and shaken slowly overnight in a flask containing M9 buffer to
- allow them to hatch. Synchronized L1s were plated onto either NGM with OP-50 or
- 746 HGM with NA22 plates as needed. Synchronized L1s were used in RNA-seq, IF, and
- 747 larval development assays. After synchronization, L1s were grown to L3, or adult as
- 748 needed per assay.

749 Auxin Treatment

- 750 Strains were subjected to auxin (Thermo Fisher Alfa Aesar Indol-3-Acetic Acid
- 751 #A10556) by incorporation into NGM or HGM plates at a final concentration of 4mM,
- as described in [42,71]. Auxin-containing plates were maintained in the dark at 4°C for
- 753 up to a month.

Assay of viability upon auxin exposure initiated during

embryogenesis

- 756 L4 hermaphrodites were placed on an auxin-containing plate to ensure all embryonic
- 757 development occurs while exposed to auxin. Plates were maintained in the dark at
- 758 20°C. Worms were placed on plates with or without auxin for an egg-laying period of 24
- hours. After this period, the adult was removed from the plate, and the embryos laid
- were counted. 24 hours later, the number of dead larvae and dead embryos were
- quantified. Live adults were counted 3 days after the initial egg-laying period. Three
- independent replicates were performed. Differences were evaluated using Fisher's
- exact test comparing the numbers of dead and live progeny for each genotype.

764 Assay of viability upon auxin exposure initiated during larval

765 **development**

- 766 Experiments testing larval development began with synchronized L1 larvae. The
- 767 synchronized population was resuspended in M9 and split evenly between an auxin
- 768 plate and a plate without auxin for 3 days. Worms surviving after 3 days were counted.
- Assuming an equal number of larvae initially plated, the final counts are reported as a
- 770 ratio of survival on auxin to survival off auxin. Three independent replicates were
- 771 performed. Differences were evaluated using Chi square test comparing the number of
- surviving worms on auxin to the number surviving off auxin of each genotype.

Brood Count Assay

Young adult hermaphrodites were allowed to lay eggs on NGM and moved to new plate each day until fertilized embryos were no longer produced. For each plate, after removal of the parent, the number of embryos laid were counted, and after 24 hours, the number of dead embryos were counted. After 3 days of development, the number of surviving adults were counted. Embryonic viability was quantified as the number of hatched embryos/total embryos. Larval viability was quantified as total number of adults/hatched embryos.

Immunofluorescence (IF)

Hermaphrodite worms were dissected in 1x sperm salts (50 mM Pipes pH 7, 25 mM KCl, 1 mM MgSO₄, 45 mM NaCl, and 2 mM CaCl₂) and fixed in 4% paraformaldehyde (PFA) diluted in 1X sperm salts on a glass slide for 5 minutes in a humid chamber containing PBS-T (PBS with 0.1% and Triton X-100). Slides were frozen on dry ice for at least 20 minutes with a 20x20 mm coverslip over the diluted PFA and dissected *C. elegans*. Using a razor blade, the coverslip was removed by flicking the coverslip off the slide. The slides were then washed in PBS-T 3 times for 10 minutes each. 30µL of diluted primary antibody was applied to each slide, a piece of parafilm was placed over the spot with the antibody to slow evaporation. The slides were incubated in a humid chamber at room temperature overnight. Slides were washed in PBS-T 3 times for 10 minutes and stained with corresponding secondary antibodies diluted 1:100 in PBS-T at 37°C for 1 hour. Three more washes in PBS-T were completed after the secondary antibody incubation. In the third wash, the nucleus was stained using DAPI diluted in PBS-T for 10 minutes at room temperature. Slides are mounted in Vectashield (Vector Labs).

Fluorescence in situ Hybridization (FISH)

Degenerate Primer PCR was used to amplify purified yeast artificial chromosomes (YACs) containing sequences corresponding to regions of the X chromosome and then labeled with dCTP-Cy3 alongside standard nucleotides using random priming as in [33,72]. The X paint FISH probe generated this way covers about 90% of the X. Adult hermaphrodites were dissected on glass slides in 1x sperm salts and fixed in 4% PFA. After 5 minutes of fixation, the specimen was covered with a 20x20 coverslip and placed on dry ice for at least 20 minutes. The coverslip was then flicked off the slide with a razor blade. Slides were washed in PBS-T three times and subjected to an ethanol series of increasing concentrations (70%, 80%, 90%, 100% EtOH) for 2 minutes each, after which the slides were air dried. To each slide, 10uL of X paint probe was added and incubated at 37°C overnight. Next day, the slides were washed in a 39°C water bath in 2x SSC/50% formamide three times, in 2X SSC solution three times for 5 minutes each, then in 1x SSC once for 10 minutes, followed by a room temperature wash in 4x SSC. DAPI was included in the final 4x SSC wash and slides were mounted using Vectashield. For FISH followed by IF, DAPI was excluded in the final 4X SSC wash, after which IF was performed as described above.

Microscopy

814

820

832

841842

- 815 Microscopy was performed using an Olympus BX61 microscope and a 60X APO oil
- 816 immersion objective. Images were taken with a Hamamatsu ORCA-ER High-Resolution
- 817 Monochrome Cooled CCD (IEEE 1394) camera. 3D images of nuclei were captured
- 818 using 0.2-micrometer Z-spacing. The nuclei presented in this study are from intestinal
- 819 cells. To observe signal depletion, exposure times were standardized to wild type.

Analysis of X Volume

- Z-stacked images of intestinal nuclei of hermaphrodites were trimmed to 10-15 slices at
- 822 0.2 µM apart to include only planes with nuclear signal. Background signal was
- subtracted in ImageJ Fiji with a rolling ball radius of 50 pixels. After splitting the
- channels, the 3dManager from the 3dSuite plugin was used to create a three-
- dimensional ROI of the DAPI signal and a three-dimensional ROI of the FISH signal in
- the Cy3 channel [73]. The area of the Cy3 channel ROI inside the DAPI ROI was then
- 827 compared in the 3dSuite 3DManager to find the X chromosome volume in the nucleus.
- The mask for the X chromosomes was limited to the area that overlaps with the DAPI
- mask signal, ensuring that the quantifications do not include non-specific staining of X
- paint FISH. The volume of the nucleus occupied is a ratio of the X signal relative to the
- 831 DAPI signal measured in voxels (volumetric pixels).

Three-Zone Assay

- 833 From the images of nuclei stained using FISH targeting the X chromosome, the middle
- 834 slice with the most in-focus FISH signal was selected. The background was subtracted
- in ImageJ FIJI with a rolling ball radius of 50 pixels. The DAPI and Cy3 channels were
- then split and thresholded. Using the native ROI manager in ImageJ FIJI, the threshold
- of the DAPI mask was used to draw three concentric ellipses that formed three zones of
- equal area in the nucleus. The Cy3 signal overlap with each zone was calculated using
- the ROI Manager to return the X chromosome FISH signal percentage in each zone.
- For this assay, only nuclei with smooth edges and an elliptical shape were used.

mRNA-seq

- 843 Synchronized L1s were placed on HGM plates with or without auxin and NA22 [74], 24-
- hours later, L3 larvae were collected in M9. After pelleting, excess M9 was removed,
- and the remaining pellet was snap-frozen in liquid nitrogen with 1mL of Trizol. RNA was
- extracted and cleaned from the collected *C. elegans* using Qiagen RNeasy Kit. Reads
- were trimmed for quality use. Poly-A enrichment, library prep, and next-generation
- 848 sequencing were conducted in the Advanced Genomics Core at the University of
- 849 Michigan. RNA was assessed for quality using the TapeStation or Bioanalyzer (Agilent).
- 850 Samples with RINs (RNA Integrity Numbers) of 8 or greater were subjected to Poly-A
- enrichment using the NEBNext Poly(A) mRNA Magnetic Isolation Module (NEB catalog
- number E7490). NEBNext Ultra II Directional RNA Library Prep Kit for Illumina (catalog
- 853 number E7760L) and NEBNext Multiplex Oligos for Illumina Unique dual (catalog
- number E6448S) were then used for library prep. The mRNA was fragmented and

- 855 copied into first-strand cDNA using reverse transcriptase and random primers. The 3'
- ends of the cDNA were then adenylated, and adapters were ligated. The PCR products
- were purified and enriched to create the final cDNA library. Qubit hsDNA (Thermofisher)
- and LabChip (Perkin Elmer) checked the final libraries for quality and quantity. The
- samples were pooled and sequenced on the Illumina NovaSeqX 10B paired-end 150bp,
- according to the manufacturer's recommended protocols. BCL Convert Conversion
- Software v4.0 (Illumina) generated de-multiplexed Fastq files. The reads were trimmed
- using CutAdapt v2.3. FastQC v0.11.8 was used to ensure the quality of data [75,76].
- Reads were mapped to the reference genome WBcel235 and read counts were
- generated using Salmon v1.9.0 [77]. Differential gene expression analysis was
- performed using DESeq2 v1.42.0 [78]. Downstream analyses were performed using R
- scripts and packages.

867

References

- 1. Ohno S. Sex Chromosomes and Sex-Linked Genes: Springer Berlin Heidelberg; 1967. doi:10.1007/978-3-642-88178-7
- Lau AC, Csankovszki G. Balancing up and downregulation of the C. elegans X
 chromosomes. Curr Opin Genet Dev. 2015;31: 50–56.
- 872 doi:10.1016/j.gde.2015.04.001
- 873 3. Madl JE, Herman RK. Polyploids and sex determination in Caenorhabditis elegans. 874 Genetics. 1979;93: 393–402.
- Nusbaum C, Meyer BJ. The Caenorhabditis Elegans Gene Sdc-2 Controls Sex Determination and Dosage Compensation in Xx Animals. Genetics. 1989;122: 579–593.
- Hodgkin J. X chromosome dosage and gene expression in Caenorhabditis
 elegans: Two unusual dumpy genes. Mol Gen Genet. 1983;192: 452–458.
 doi:10.1007/BF00392190
- 881 6. Meyer BJ, Casson LP. Caenorhabditis elegans compensates for the difference in X chromosome dosage between the sexes by regulating transcript levels. Cell. 1986;47: 871–881. doi:10.1016/0092-8674(86)90802-0
- Hirano T. Condensins: organizing and segregating the genome. Curr Biol CB. 2005;15: R265-275. doi:10.1016/j.cub.2005.03.037
- 886 8. Ganji M, Shaltiel IA, Bisht S, Kim E, Kalichava A, Haering CH, et al. Real-time imaging of DNA loop extrusion by condensin. Science. 2018;360: 102–105. doi:10.1126/science.aar7831
- Kong M, Cutts EE, Pan D, Beuron F, Kaliyappan T, Xue C, et al. Human
 Condensin I and II Drive Extensive ATP-Dependent Compaction of Nucleosome-Bound DNA. Mol Cell. 2020;79: 99-114.e9. doi:10.1016/j.molcel.2020.04.026

- Hirano T. Condensins: universal organizers of chromosomes with diverse functions. Genes Dev. 2012;26: 1659–1678. doi:10.1101/gad.194746.112
- 11. Csankovszki G, Collette K, Spahl K, Carey J, Snyder M, Petty E, et al. Three
 distinct condensin complexes control C. elegans chromosome dynamics. Curr Biol.
 2009;19: 9–19. doi:10.1016/j.cub.2008.12.006
- 897 12. Mets DG, Meyer BJ. Condensins Regulate Meiotic DNA Break Distribution, thus 898 Crossover Frequency, by Controlling Chromosome Structure. Cell. 2009;139: 73– 899 86. doi:10.1016/j.cell.2009.07.035
- Hirano T, Kobayashi R, Hirano M. Condensins, chromosome condensation protein complexes containing XCAP-C, XCAP-E and a Xenopus homolog of the Drosophila Barren protein. Cell. 1997;89: 511–521. doi:10.1016/s0092-8674(00)80233-0
- 904 14. Paul MR, Hochwagen A, Ercan S. Condensin action and compaction. Curr Genet. 2019;65: 407–415. doi:10.1007/s00294-018-0899-4
- 906 15. Chuang PT, Albertson DG, Meyer BJ. DPY-27:a chromosome condensation protein homolog that regulates C. elegans dosage compensation through association with the X chromosome. Cell. 1994;79: 459–474. doi:10.1016/0092-8674(94)90255-0
- Hagstrom KA, Holmes VF, Cozzarelli NR, Meyer BJ. C. elegans condensin
 promotes mitotic chromosome architecture, centromere organization, and sister
 chromatid segregation during mitosis and meiosis. Genes Dev. 2002;16: 729–742.
 doi:10.1101/gad.968302
- 17. Lau AC, Nabeshima K, Csankovszki G. The C. elegans dosage compensation
 915 complex mediates interphase X chromosome compaction. Epigenetics Chromatin.
 916 2014;7: 31. doi:10.1186/1756-8935-7-31
- 18. Lau AC, Csankovszki G. Condensin-mediated chromosome organization and gene
 regulation. Front Genet. 2014;5: 473. doi:10.3389/fgene.2014.00473
- 919 19. Crane E, Bian Q, McCord RP, Lajoie BR, Wheeler BS, Ralston EJ, et al. Condensin-driven remodelling of X chromosome topology during dosage compensation. Nature. 2015;523: 240–244. doi:10.1038/nature14450
- 922 20. Kim J, Jimenez DS, Ragipani B, Zhang B, Street LA, Kramer M, et al. Condensin
 923 DC loads and spreads from recruitment sites to create loop-anchored TADs in C.
 924 elegans. Tyler JK, editor. eLife. 2022;11: e68745. doi:10.7554/eLife.68745
- 21. Chu DS, Dawes HE, Lieb JD, Chan RC, Kuo AF, Meyer BJ. A molecular link
 between gene-specific and chromosome-wide transcriptional repression. Genes
 Dev. 2002;16: 796–805. doi:10.1101/gad.972702

- 928 22. Yonker SA, Meyer BJ. Recruitment of C. elegans dosage compensation proteins for gene-specific versus chromosome-wide repression. Development. 2003;130:
- 930 6519–6532. doi:10.1242/dev.00886
- 931 23. Pferdehirt RR, Meyer BJ. SUMOylation is essential for sex-specific assembly and
- 932 function of the Caenorhabditis elegans dosage compensation complex on X
- 933 chromosomes. Proc Natl Acad Sci. 2013;110: E3810–E3819.
- 934 doi:10.1073/pnas.1315793110
- 24. Kruesi WS, Core LJ, Waters CT, Lis JT, Meyer BJ. Condensin controls recruitment
 936 of RNA polymerase II to achieve nematode X-chromosome dosage compensation.
- 937 Elife. 2013;2: e00808. doi:10.7554/eLife.00808
- 938 25. Brejc K, Bian Q, Uzawa S, Wheeler BS, Anderson EC, King DS, et al. Dynamic
 939 Control of X Chromosome Conformation and Repression by a Histone H4K20
 940 Demethylase. Cell. 2017;171: 85-102.e23. doi:10.1016/j.cell.2017.07.041
- 941 26. Wells MB, Snyder MJ, Custer LM, Csankovszki G. Caenorhabditis elegans dosage
 942 compensation regulates histone H4 chromatin state on X chromosomes. Mol Cell
 943 Biol. 2012;32: 1710–1719. doi:10.1128/MCB.06546-11
- Vielle A, Lang J, Dong Y, Ercan S, Kotwaliwale C, Rechtsteiner A, et al.
 H4K20me1 contributes to downregulation of X-linked genes for C. elegans dosage compensation. PLoS Genet. 2012;8: e1002933. doi:10.1371/journal.pgen.1002933
- 947 28. Breimann L, Morao AK, Kim J, Sebastian Jimenez D, Maryn N, Bikkasani K, et al.
 948 The histone H4 lysine 20 demethylase DPY-21 regulates the dynamics of
 949 condensin DC binding. J Cell Sci. 2022;135: jcs258818. doi:10.1242/jcs.258818
- 29. Kramer M, Kranz A-L, Su A, Winterkorn LH, Albritton SE, Ercan S. Developmental
 Dynamics of X-Chromosome Dosage Compensation by the DCC and H4K20me1
 in C. elegans. PLoS Genet. 2015;11: e1005698. doi:10.1371/journal.pgen.1005698
- 30. Towbin BD, González-Aguilera C, Sack R, Gaidatzis D, Kalck V, Meister P, et al. Step-wise methylation of histone H3K9 positions heterochromatin at the nuclear periphery. Cell. 2012;150: 934–947. doi:10.1016/j.cell.2012.06.051
- 31. Ikegami K, Egelhofer TA, Strome S, Lieb JD. Caenorhabditis elegans chromosome
 957 arms are anchored to the nuclear membrane via discontinuous association with
 958 LEM-2. Genome Biol. 2010;11: R120. doi:10.1186/gb-2010-11-12-r120
- 32. Gonzalez-Sandoval A, Towbin BD, Kalck V, Cabianca DS, Gaidatzis D, Hauer MH,
 960 et al. Perinuclear Anchoring of H3K9-Methylated Chromatin Stabilizes Induced Cell
 961 Fate in C. elegans Embryos. Cell. 2015;163: 1333–1347.
 962 doi:10.1016/j.cell.2015.10.066
- 33. Snyder MJ, Lau AC, Brouhard EA, Davis MB, Jiang J, Sifuentes MH, et al.
 Anchoring of Heterochromatin to the Nuclear Lamina Reinforces Dosage

- Compensation-Mediated Gene Repression. PLoS Genet. 2016;12: e1006341. doi:10.1371/journal.pgen.1006341
- 967 34. Dawes HE, Berlin DS, Lapidus DM, Nusbaum C, Davis TL, Meyer BJ. Dosage compensation proteins targeted to X chromosomes by a determinant of hermaphrodite fate. Science. 1999;284: 1800–1804.
- 35. Meyer BJ. Targeting X chromosomes for repression. Curr Opin Genet Dev.
 2010;20: 179–189. doi:10.1016/j.gde.2010.03.008
- 36. Custer LM, Snyder MJ, Flegel K, Csankovszki G. The onset of C. elegans dosage
 compensation is linked to the loss of developmental plasticity. Dev Biol. 2014;385:
 279–290. doi:10.1016/j.ydbio.2013.11.001
- 37. Yuzyuk T, Fakhouri THI, Kiefer J, Mango SE. The polycomb complex protein mes 2/E(z) promotes the transition from developmental plasticity to differentiation in C.
 elegans embryos. Dev Cell. 2009;16: 699–710. doi:10.1016/j.devcel.2009.03.008
- 38. Sulston JE, Schierenberg E, White JG, Thomson JN. The embryonic cell lineage of
 the nematode Caenorhabditis elegans. Dev Biol. 1983;100: 64–119.
 doi:10.1016/0012-1606(83)90201-4
- 981 39. Plenefisch JD, DeLong L, Meyer BJ. Genes that implement the hermaphrodite
 982 mode of dosage compensation in Caenorhabditis elegans. Genetics. 1989;121:
 983 57–76. doi:10.1093/genetics/121.1.57
- 984 40. Cabianca DS, Muñoz-Jiménez C, Kalck V, Gaidatzis D, Padeken J, Seeber A, et
 985 al. Active chromatin marks drive spatial sequestration of heterochromatin in C.
 986 elegans nuclei. Nature. 2019;569: 734–739. doi:10.1038/s41586-019-1243-y
- 41. Li Q, Kaur A, Mallory B, Hariri S, Engebrecht J. Inducible degradation of dosage compensation protein DPY-27 facilitates isolation of *Caenorhabditis elegans* males for molecular and biochemical analyses. Ward J, editor. G3
 GenesGenomesGenetics. 2022;12: jkac085. doi:10.1093/g3journal/jkac085
- 291 42. Zhang L, Ward JD, Cheng Z, Dernburg AF. The auxin-inducible degradation (AID)
 system enables versatile conditional protein depletion in C. elegans. Development.
 2015;142: 4374–4384. doi:10.1242/dev.129635
- 994 43. Hedgecock EM, White JG. Polyploid tissues in the nematode *Caenorhabditis* elegans. Dev Biol. 1985;107: 128–133. doi:10.1016/0012-1606(85)90381-1
- 44. Kelly WG, Schaner CE, Dernburg AF, Lee M-H, Kim SK, Villeneuve AM, et al. X-chromosome silencing in the germline of C. elegans. Dev Camb Engl. 2002;129: 479–492.

- 999 45. Crittenden SL, Leonhard KA, Byrd DT, Kimble J. Cellular Analyses of the Mitotic Region in the Caenorhabditis elegans Adult Germ Line. Mol Biol Cell. 2006;17: 1000 3051-3061. doi:10.1091/mbc.E06-03-0170
- 1001
- 1002 46. Schiksnis EC, Nicholson AL, Modena MS, Pule MN, Arribere JA, Pasquinelli AE. 1003 Auxin-independent depletion of degron-tagged proteins by TIR1. MicroPublication
- 1004 Biol. 2020: 10.17912/micropub.biology.000213.
- 1005 doi:10.17912/micropub.biology.000213
- 1006 47. Natsume T, Kiyomitsu T, Saga Y, Kanemaki MT. Rapid Protein Depletion in Human Cells by Auxin-Inducible Degron Tagging with Short Homology Donors. 1007
- Cell Rep. 2016;15: 210-218. doi:10.1016/j.celrep.2016.03.001 1008
- 1009 48. Martinez MA, Kinney BA, Medwig-Kinney TN, Ashley G, Ragle JM, Johnson L, et 1010 al. Rapid degradation of Caenorhabditis elegans proteins at single-cell resolution 1011 with a synthetic auxin. G3 Genes Genomes Genet. 2020;10: 267-280.
- 1012 49. Samejima K, Booth DG, Ogawa H, Paulson JR, Xie L, Watson CA, et al. Functional 1013 analysis after rapid degradation of condensins and 3D-EM reveals chromatin 1014 volume is uncoupled from chromosome architecture in mitosis. J Cell Sci.
- 1015 2018;131: jcs210187. doi:10.1242/jcs.210187
- 1016 50. Hirano T, Mitchison TJ. A heterodimeric coiled-coil protein required for mitotic 1017 chromosome condensation in vitro. Cell. 1994;79: 449-458. doi:10.1016/0092-1018 8674(94)90254-2
- 1019 51. Houlard M, Godwin J, Metson J, Lee J, Hirano T, Nasmyth K. Condensin confers 1020 the longitudinal rigidity of chromosomes. Nat Cell Biol. 2015;17: 771–781. 1021 doi:10.1038/ncb3167
- 1022 52. Piskadlo E, Tavares A, Oliveira RA. Metaphase chromosome structure is dynamically maintained by condensin I-directed DNA (de)catenation. eLife. 2017;6: 1023 1024 e26120. doi:10.7554/eLife.26120
- 1025 53. Zhiteneva A, Bonfiglio JJ, Makarov A, Colby T, Vagnarelli P, Schirmer EC, et al. Mitotic post-translational modifications of histones promote chromatin compaction 1026 1027 in vitro. Open Biol. 2017;7: 170076. doi:10.1098/rsob.170076
- 1028 54. Corvalan AZ, Coller HA. Methylation of histone 4's lysine 20: a critical analysis of 1029 the state of the field. Physiol Genomics. 2021;53: 22-32. doi:10.1152/physiolgenomics.00128.2020 1030
- 1031 55. Wilkins BJ, Rall NA, Ostwal Y, Kruitwagen T, Hiragami-Hamada K, Winkler M, et al. A cascade of histone modifications induces chromatin condensation in mitosis. 1032 1033 Science. 2014;343: 77-80. doi:10.1126/science.1244508
- 1034 56. Javasky E, Shamir I, Gandhi S, Egri S, Sandler O, Rothbart SB, et al. Study of mitotic chromatin supports a model of bookmarking by histone modifications and 1035

- reveals nucleosome deposition patterns. Genome Res. 2018;28: 1455–1466.
- 1037 doi:10.1101/gr.230300.117
- 1038 57. Methot SP, Padeken J, Brancati G, Zeller P, Delaney CE, Gaidatzis D, et al.
- 1039 H3K9me selectively blocks transcription factor activity and ensures differentiated
- 1040 tissue integrity. Nat Cell Biol. 2021;23: 1163–1175. doi:10.1038/s41556-021-
- 1041 00776-w
- 1042 58. Anderson EC, Frankino PA, Higuchi-Sanabria R, Yang Q, Bian Q, Podshivalova K,
- et al. X Chromosome Domain Architecture Regulates Caenorhabditis elegans
- Lifespan but Not Dosage Compensation. Dev Cell. 2019;51: 192-207.e6.
- 1045 doi:10.1016/j.devcel.2019.08.004
- 1046 59. Csankovszki G, Panning B, Bates B, Pehrson JR, Jaenisch R. Conditional deletion
- of Xist disrupts histone macroH2A localization but not maintenance of X
- 1048 inactivation. Nat Genet. 1999;22: 323–324. doi:10.1038/11887
- 1049 60. Csankovszki G, Nagy A, Jaenisch R. Synergism of Xist RNA, DNA methylation,
- and histone hypoacetylation in maintaining X chromosome inactivation. J Cell Biol.
- 1051 2001;153: 773–783. doi:10.1083/jcb.153.4.773
- 1052 61. Heard E, Disteche CM. Dosage compensation in mammals: fine-tuning the
- expression of the X chromosome. Genes Dev. 2006;20: 1848–1867.
- 1054 doi:10.1101/gad.1422906
- 1055 62. Leonhardt H, Page AW, Weier HU, Bestor TH. A targeting sequence directs DNA
- methyltransferase to sites of DNA replication in mammalian nuclei. Cell. 1992;71:
- 1057 865–873. doi:10.1016/0092-8674(92)90561-p
- 1058 63. Audergon PNCB, Catania S, Kagansky A, Tong P, Shukla M, Pidoux AL, et al.
- 1059 Epigenetics. Restricted epigenetic inheritance of H3K9 methylation. Science.
- 1060 2015;348: 132–135. doi:10.1126/science.1260638
- 1061 64. Margueron R, Justin N, Ohno K, Sharpe ML, Son J, Drury III WJ, et al. Role of the
- polycomb protein EED in the propagation of repressive histone marks. Nature.
- 1063 2009;461: 762–767. doi:10.1038/nature08398
- 1064 65. Hansen KH, Bracken AP, Pasini D, Dietrich N, Gehani SS, Monrad A, et al. A
- model for transmission of the H3K27me3 epigenetic mark. Nat Cell Biol. 2008;10:
- 1066 1291–1300. doi:10.1038/ncb1787
- 1067 66. Liu W, Tanasa B, Tyurina OV, Zhou TY, Gassmann R, Liu WT, et al. PHF8
- mediates histone H4 lysine 20 demethylation events involved in cell cycle
- 1069 progression. Nature. 2010;466: 508–512. doi:10.1038/nature09272
- 1070 67. Brenner S. The genetics of Caenorhabditis elegans. Genetics. 1974;77: 71–94.

- 1071 68. Zhang S. Cell isolation and culture. WormBook. 2013; 1–39. doi:10.1895/wormbook.1.157.1 1072 1073 69. Porta-de-la-Riva M, Fontrodona L, Villanueva A, Cerón J. Basic Caenorhabditis 1074 elegans Methods: Synchronization and Observation. J Vis Exp JoVE. 2012; 4019. 1075 doi:10.3791/4019 1076 70. M9 Buffer for Worms. Cold Spring Harb Protoc. 2014;2014; pdb.rec081315. 1077 doi:10.1101/pdb.rec081315 1078 71. Ashley GE, Duong T, Levenson MT, Martinez MAQ, Johnson LC, Hibshman JD, et al. An expanded auxin-inducible degron toolkit for Caenorhabditis elegans. 1079 1080 Greenstein D, editor. Genetics. 2021;217: iyab006. doi:10.1093/genetics/iyab006 1081 72. Nabeshima K, Mlynarczyk-Evans S, Villeneuve AM. Chromosome Painting Reveals Asynaptic Full Alignment of Homologs and HIM-8-Dependent Remodeling 1082 1083 of X Chromosome Territories during Caenorhabditis elegans Meiosis, PLoS Genet. 1084 2011;7: e1002231. doi:10.1371/journal.pgen.1002231 1085 73. Ollion J, Cochennec J, Loll F, Escudé C, Boudier T. TANGO: a generic tool for 1086 high-throughput 3D image analysis for studying nuclear organization. Bioinforma 1087 Oxf Engl. 2013;29: 1840-1841. doi:10.1093/bioinformatics/btt276 1088 74. Zhang S, Kuhn JR. Cell isolation and culture. WormBook: The Online Review of C 1089 elegans Biology [Internet]. WormBook; 2018. Available: 1090 https://www.ncbi.nlm.nih.gov/books/NBK153594/ 1091 75. Martin M. Cutadapt removes adapter sequences from high-throughput sequencing 1092 reads. EMBnet.journal. 2011;17: 10-12. doi:10.14806/ej.17.1.200 1093 76. FastQC. 2015. Available: https://gubeshub.org/resources/fastqc
- 1094 77. Patro R, Duggal G, Love MI, Irizarry RA, Kingsford C. Salmon provides fast and bias-aware quantification of transcript expression. Nat Methods. 2017;14: 417–419. doi:10.1038/nmeth.4197
- 1097 78. Love MI, Huber W, Anders S. Moderated estimation of fold change and dispersion for RNA-seq data with DESeq2. Genome Biol. 2014;15: 550. doi:10.1186/s13059-014-0550-8

Supporting information

1102 **S1** Fig. Comparison of all rings from the three-zone assay of X localization within the nucleus with and without auxin treatment. (A) Three-zone assay for the X paint FISH signal (n = 20 nuclei) in strains grown without auxin showing all three concentric

zones. **(B)** Three-zone assay for the X paint FISH signal (n = 20 nuclei) in strains grown

1106 in the presence of auxin.

- 1107 S2 Fig. mRNA-seq analysis of dpy-27::AID strains. (A-D) Boxplots depicting the
- 1108 distribution of the expression difference of X-linked genes and expression difference of
- 1109 genes on autosomes. Gene expression is plotted as the log2 ratio of the strains being
- 1110 compared. Statistical significance is determined by the differences in gene expression
- between the X and autosomes by a Wilcoxon rank-sum test. (n.s. = not significant, * = p
- 1112 < 0.05, ** = p<0.01, *** = p < 0.001) (E) Principal component analysis (PCA) plot
- depicting the relationships among TIR1; dpy-27::AID, and TIR1; dpy-27::AID; cec-4.
- 1114 Auxin treatment is indicated alongside the corresponding genotype in the figure.
- 1115 S3 Fig. RNA seq analysis of cec-4 and dpy-21 mutants. Principal component
- 1116 analysis (PCA) plot depicting the relationships among wild-type, single mutants (cec-4
- and *dpy-21*), and double mutants (*cec-4*; *dpy-21*) based on gene expression profiles.
- 1118 S1 File. Statistical analysis of the survival of embryo in the presence or absence
- 1119 **of auxin.**
- 1120 S2 File. Statistical analysis of the survival of larvae in the presence or absence of
- 1121 auxin.
- 1122 S3 File. Statistical analysis of X chromosome decondensation.
- 1123 S4 File. Statistical analysis of X chromosome localization within the nucleus via
- 1124 the three-zone assay.
- 1125 S5 File. Statistical analysis of mRNA-seq.
- 1126 S6 File. Statistical analysis of the broods laid by worms containing cec-4 and dpy-
- 1127 **21** mutations.

- 1128 S7 File. Statistical analysis of the decondensation of the X chromosome in cec-4
- 1129 and *dpy-21* containing mutants.